Palaeogeography, Palaeoclimatology, Palaeoecology 610 (2023) 111344

Contents lists available at ScienceDirect

Palaeogeography, Palaeoclimatology, Palaeoecology

journal homepage: www.elsevier.com/locate/palaeo

More gaps than record! A new look at the Pliensbachian/Toarcian boundary event guided by coupled chemo-sequence stratigraphy

Stéphane Bodin [a,*], Alicia Fantasia [a,b], Francois-Nicolas Krencker [a,c], Bjarke Nebsbjerg [a], Lasse Christiansen [a], Simon Andrieu [a,d]

[a] Department of Geoscience, Aarhus University, Høegh-Guldbergs Gade 2, 8000 Aarhus C, Denmark
[b] Université de Lyon, UCBL, ENSL, UJM, CNRS, LGL-TPE, F-69622 Villeurbanne, France
[c] Leibniz Universität Hannover, Institut für Geologie, Callinstraße 30, 30167 Hannover, Germany
[d] BRGM-French Geological Survey, 3 avenue Claude Guillemin, BP 36009, 45060 Orléans, France

ARTICLE INFO

Editor: Dr. A Dickson

Keywords:
Carbonate factory demise
Carbon isotopes
Pliensbachian
Toarcian
Hiatus
South-East France Basin

ABSTRACT

The Pliensbachian/Toarcian boundary (Pl/To) event precedes by ca. 1 Myr the onset of the Toarcian Oceanic Anoxic Event. It corresponds to a second order mass extinction associated with an outstanding collapse of shallow marine ecosystems at global scale. Yet, our knowledge about its exact driver(s) and unfolding is relatively ambiguous due to the numerous hiatuses present in the sedimentary record during this critical time interval. In this study, an integrated carbon isotope chemostratigraphy and sequence stratigraphy approach is applied to two case studies (the upper Pliensbachian in South-East France and the Pliensbachian–Toarcian transition in Morocco) to demonstrate how the major changes in sea-level and sedimentation supply accompanying the Pl/To event led to the formation of ubiquitous, often cryptic hiatal surfaces in the sedimentary record. Hence, as a consequence of strongly progradational stacking pattern during the latest Pliensbachian related to a global sea-level lowstand associated with cold greenhouse climate, proximal settings were characterized by bypass and/or erosion, inducing an incomplete record of the Spinatum chronozone in localities situated in the outer part of sedimentary basins. In the earliest Toarcian, the collapse of the neritic carbonate factory led to a halt of carbonate mud export into the basin, resulting in sediment starvation in most basins characterized by a carbonate-dominated sedimentation regime before the environmental perturbation. Only localities where vigorous siliciclastic sediment supply took over are likely to have a more complete sedimentary record of the immediate aftermath of the carbonate production collapse. This combination of causes explains the ubiquitous incompleteness of the record of the Pliensbachian/Toarcian transition in numerous European localities where the bulk of our current understanding about the Pl/To event derives from. A comparison between the two known most expanded and complete records of the Pliensbachian–Toarcian transition of the Llanbedr (Mochras Farm) core in Wales and Bou Oumardoul n'Imazighn section in Morocco shows that the onset of the environmental perturbations is associated with a positive carbon isotope excursion spanning the Pliensbachian/Toarcian boundary. This is followed by a negative carbon isotope excursion during the earliest Toarcian that coincides with the global collapse of neritic carbonate factory and an ample sea-level fall.

1. Introduction

The late Early Jurassic has experienced one of the most severe environmental perturbations of the Mesozoic, leading to a 2nd-order mass extinction event affecting both pelagic and benthic organisms (Little and Benton, 1995; Dera et al., 2010; Caruthers et al., 2013; Danise et al., 2013; Vasseur et al., 2021). Due to presence of organic matter-rich deposits and a large negative carbon isotope excursion in the lower Toarcian *levisoni* zone (Hesselbo et al., 2007; Jenkyns, 2010; Suan et al., 2010), the Toarcian Oceanic Anoxic Event (T-OAE) is the most iconic expression of this Early Jurassic environmental perturbation, and has hence been the focus of numerous studies (e.g. Jenkyns, 1988; Hesselbo et al., 2000, 2007; Röhl and Schmid-Röhl, 2005; van de Schootbrugge et al., 2005; Hermoso et al., 2009; French et al., 2014). In the last decade, many studies have pointed at the fact that the T-OAE is actually the climax of a long-lasting early Toarcian event, itself inscribed within a

* Corresponding author.
E-mail address: stephane.bodin@geo.au.dk (S. Bodin).

https://doi.org/10.1016/j.palaeo.2022.111344
Received 12 August 2022; Received in revised form 15 November 2022; Accepted 28 November 2022
Available online 2 December 2022

protracted time interval of environmental perturbations starting in the late Pliensbachian and ending in the middle Toarcian (Suan et al., 2010; Dera et al., 2011; Krencker et al., 2014; Silva and Duarte, 2015; Xu et al., 2018; Baghli et al., 2020; Storm et al., 2020). Of importance here is that the early Toarcian mass extinction event is a two-fold event, with a first episode occurring at the Pliensbachian/Toarcian (Pl/To) boundary, and a second one at the onset of the T-OAE (Little and Benton, 1995; Cecca and Macchioni, 2004). Of these two episodes, the Pl/To event is the one that had the strongest impact on the biosphere (Dera et al., 2010; Caruthers et al., 2013; Brame et al., 2019; Vasseur et al., 2021), inducing a global collapse of pelagic and neritic carbonate production (Dromart et al., 1996; Suan et al., 2010; Menini et al., 2019; Krencker et al., 2020).

Yet, due to the scientific tropism toward the T-OAE, the Pl/To event has received considerably less attention, leaving numerous questions about its driver(s) unresolved. According to the current state of understanding, the Pl/To event should be characterized by a negative carbon isotope excursion spanning the Pl/To boundary (Littler et al., 2010), signalling a perturbation of the carbon cycle leading to global warming (Suan et al., 2010; Baghli et al., 2020; Ruebsam et al., 2020), and increased continental weathering (Bodin et al., 2010; Percival et al., 2016; Krencker et al., 2020). The ultimate driver of this event is not precisely known, but evidence from mercury (Hg) anomalies around this boundary (Percival et al., 2015) suggest a volcanic trigger, often equated to a first pulse of the Karoo-Ferrar Large Igneous Province (LIP). This link is however challenged by the suggestion that Hg anomalies are linked to terrestrial sedimentary flux rather than a direct proxy for volcanism (Them et al., 2019).

In this study, we will build on the pioneer work of Morard et al. (2003) who have suggested the frequent presence of hiatus spanning the Pl/To boundary in North-West European section (see also Ruebsam and Al-Husseini, 2020). By combining high-resolution carbon isotope chemostratigraphy and sequence stratigraphy from two case studies (South-East France Basin and Central High Atlas Basin of Morocco), we show and discuss how the major sediment supply and sea-level changes related to the Pl/To environmental perturbations led to the formation of ubiquitous, often cryptic, condensation and hiatus in the sedimentary record. In details, the example of the South-East France Basin will highlight how strong progradational stacking patterns linked to a long-term sea-level lowstand the end of the Pliensbachian accounts for the incompleteness of the upper *spinatum* chronozone in numerous sections. Thereafter, the example of the Central High Atlas Basin will underline how the collapse of the neritic carbonate factory in the earliest Toarcian, combined to an important short-term sea-level fall led to sediment starvation or bypass in numerous basins.

This study suggests that most of the classical localities from which the bulk of our understanding of the Pl/To event derives from (e.g., Hawsker Bottoms in England, Peniche in Portugal, Sancerre core in France, La Cerradura in Spain) are likely uncomplete, implying erroneous chronostratigraphic attribution and therefore erroneous interpretation of environmental change across the Pl/To boundary. Combining the available carbon isotope geochemical dataset from the highly-expanded records of the Dades Valley in Morocco and the Llanbedr (Mochras Farm) core in Wales (hereafter Mochras core), we will propose a new look at the carbon cycle and environmental changes during one of the most severe mass extinction events of the Mesozoic.

2. Geological settings

This study relies on new sedimentological and geochemical data from the South-East France Basin and the Central High Atlas Basin of Morocco. In France, five sedimentary sections were investigated, with a focus on the late Pliensbachian sea-level and carbon cycle changes. In Morocco, a new geochemical dataset from the Bou Oumardoul n'Imazighn composite section (Dades Valley) was established.

2.1. South-East France Basin

A total of 5 sections were investigated in the South-East France Basin (Arnaud, 2005): Barles, La Reine Jeanne, Rochebrune, Le Mousteiret, and La Baume. These sections are currently situated within the south-western part of the Dauphinois domain in the French Alps, in the vicinity of the town of Digne-les-Bains for the four first, and close to the town of Castellane for the last (Fig. 1). The Barles section is preserved in a para-autochtonous position below the Digne thrust sheet in the "écaille de Valoire" (Gidon and Pairis, 1992). La Reine Jeanne and Le Mousteiret sections are situated in the main unit of the Digne thrust sheet, whereas the Rochebrune section is situated in one of its sub-units, called La Robine unit. This latter is separated from the Digne thrust sheet by the Bès dextral strike-slip fault (Gidon, 1997; Célini et al., 2020). The La Baume section is situated in the south-westernmost part of the Digne thrust sheet. Palinspastic reconstruction, taking into account the ca. 20 km southwestward displacement of the Digne thrust sheet during the alpine orogenesis (Gidon and Pairis, 1992; Lickorish and Ford, 1998), indicates that these five sections were distributed along a ca. 30 km-long proximal-distal transect. The most proximal site was la Baume, followed by Barles, Reine Jeanne and Rochebrune sections, and finally the Le Mousteiret section, which represents the most distal setting studied here.

Biostratigraphic dating of the studied sections is based on ammonites, which are frequent throughout the studied interval (Coadou et al., 1971; de Graciansky et al., 1982, 1993; Haccard et al., 1989; Floquet et al., 2003; De Baets et al., 2008). No formal lithostratigraphic division has yet been established for the Mesozoic of the SE France Basin. Regionally, the lower Pliensbachian (also known as Carixian in France) is characterized by cliff-forming limestones containing in some place abundant chert nodules (Sup_Mat: Fig. S1), and often capped by a phosphate-rich hardground crust. The upper Pliensbachian (also called Domerian in France) is characterized by mixed limestone-marl sedimentation. The Upper Pliensbachian is typically divided into two lithostratigraphic parts: a marl-dominated lower part informally referred to as the "Marnes noires" unit, and a limestone-dominated upper part informally referred to as the "Calcaires roux" unit (Sup_Mat: Fig. S2). A phosphate-rich crust associated with a pronounced hardground and erosive/dissolution surface marks the top of the Pliensbachian. The lower to middle Toarcian is often absent or highly condensed in the Digne-les-Bains region but, when present, the lower Toarcian is dominated by black marl deposits, whereas the middle Toarcian is more carbonate-rich (e.g., Floquet et al., 2003). Finally, the upper Toarcian is characterized by thick black marl deposits rich in phosphate nodules (de Graciansky et al., 1982; Haccard et al., 1989), overlaid by Aalenian carbonate-rich deposits (Caloo, 1970; Fantasia et al., 2022).

2.2. Central High Atlas Basin, Morocco

The Central High Atlas basin is part of an aulacogen rift system formed during the Early Jurassic opening of the North Atlantic Ocean. The basin was active during the Mesozoic and early Cenozoic, before its inversion due to Alpine compression (Frizon de Lamotte et al., 2008). During the Jurassic, the basin was open on its eastern side toward the Tethys Ocean and separated from the North Atlantic Ocean by the Moroccan Meseta. The Jurassic is mostly made of carbonate-dominated sediments produced by vigorous shallow marine platform surrounding the southern and western side of the basin, that are episodically interrupted by siliciclastic-dominated sediments associated with the environmental perturbations of the Toarcian (Wilmsen and Neuweiler, 2008; Krencker et al., 2020) and the Bajocian (Bodin et al., 2017).

In the Central High Atlas Basin, the Pliensbachian is characterized by thick carbonate platform deposits (from proximal to distal: Aganane, Choucht, and Aberdouz Formations) and the basinal limestone-marl alternations of the Ouchbis Formation (Krencker et al., 2020). The Pliensbachian – Toarcian transition is characterized by declining

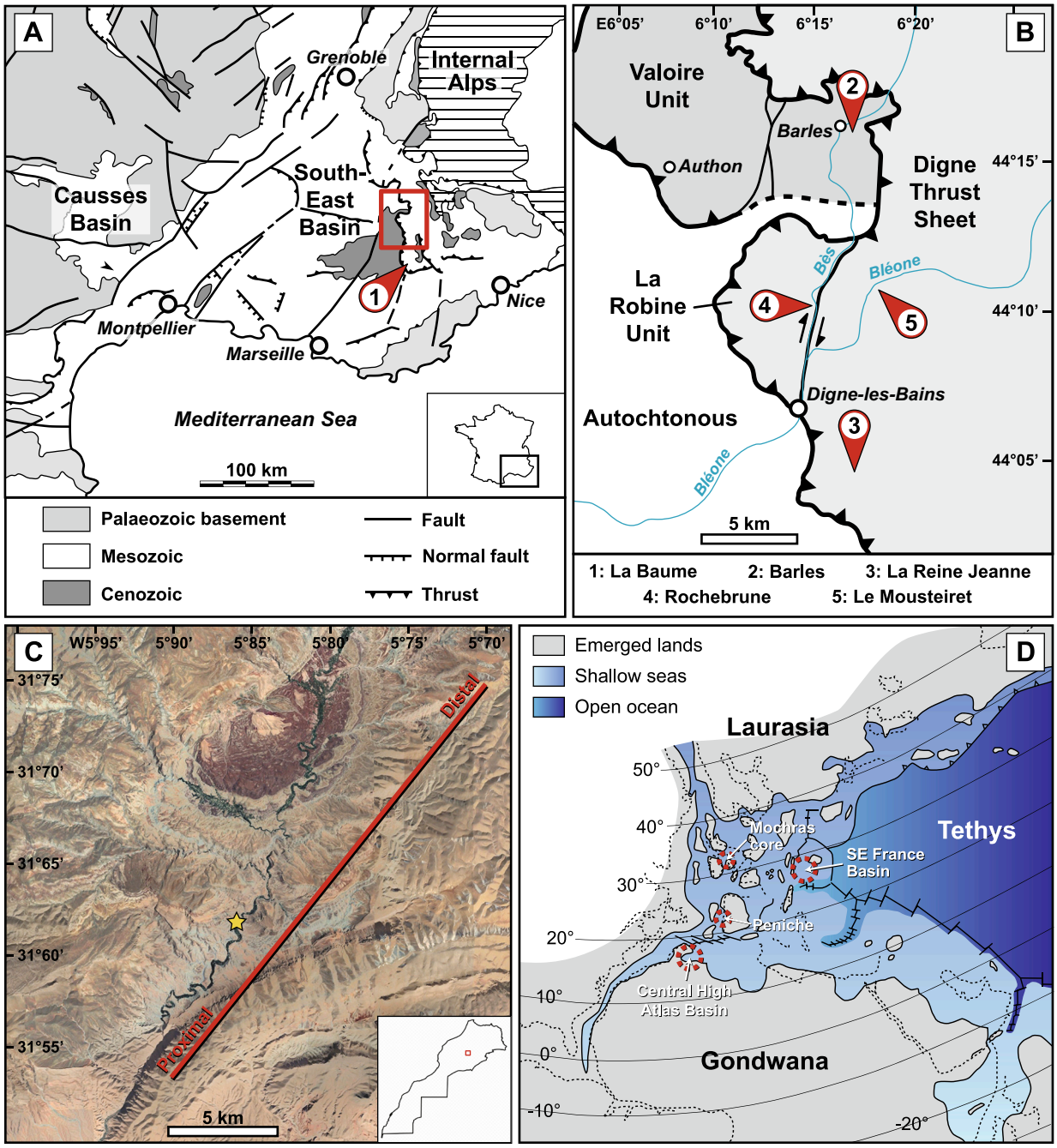

Fig. 1. Geologic and (paleo-)geographic maps showing the locations of the SE France and Moroccan sections. A. Simplified geologic map of SE France (map modified after Hamon and Merzeraud, 2007). B. Close-up view on the Digne-les-Bains area (map modified after Célini et al., 2020). C. Aerial photograph of the Dades Valley region from Google Earth. The yellow star shows the location of the Bou Oumardoul n'Imazighn section. The red line indicates the proximal–distal transect displayed in Fig. 11. Exact location of all the studied sections in the Dades Valley are given in Krencker et al. (2020, 2022). D. Paleogeographic map of the western Tethys realm showing the location of the SE France Basin and the Central High Atlas Basin, as well as the Llanbedr (Mochras Farm) core and Peniche section (modified after Bassoulet et al., 1993). (For interpretation of the references to color in this figure legend, the reader is referred to the web version of this article.)

carbonate production due to the onset of the Pl/To environmental perturbation (Wilmsen and Neuweiler, 2008; Krencker et al., 2020; Andrieu et al., 2022). A switch to siliciclastic-dominated deposits (Tagoudite Formation) characterizes the lowermost Toarcian (lower *Dactylioceras polymorphum* zone). This marked change in sedimentation has been linked to a complete demise of carbonate production (Blomeier and Reijmer, 1999; Wilmsen and Neuweiler, 2008; Bodin et al., 2016; Krencker et al., 2020) induced by combined siliciclastic poisoning and sea-level fall (Krencker et al., 2022). Mixed siliciclastic-carbonate deposits of the Tafraout Formation characterize the upper *polymorphum* and *levisoni* zones.

3. Methods

3.1. Studied sections

3.1.1. South-East France Basin

The La Baume section is located above the waterfall situated 200 m east of the La Baume village, approximately 5 km north of the town of Castellane (N44°53′36″, E6°30′07″; Fig. 2). According to the local

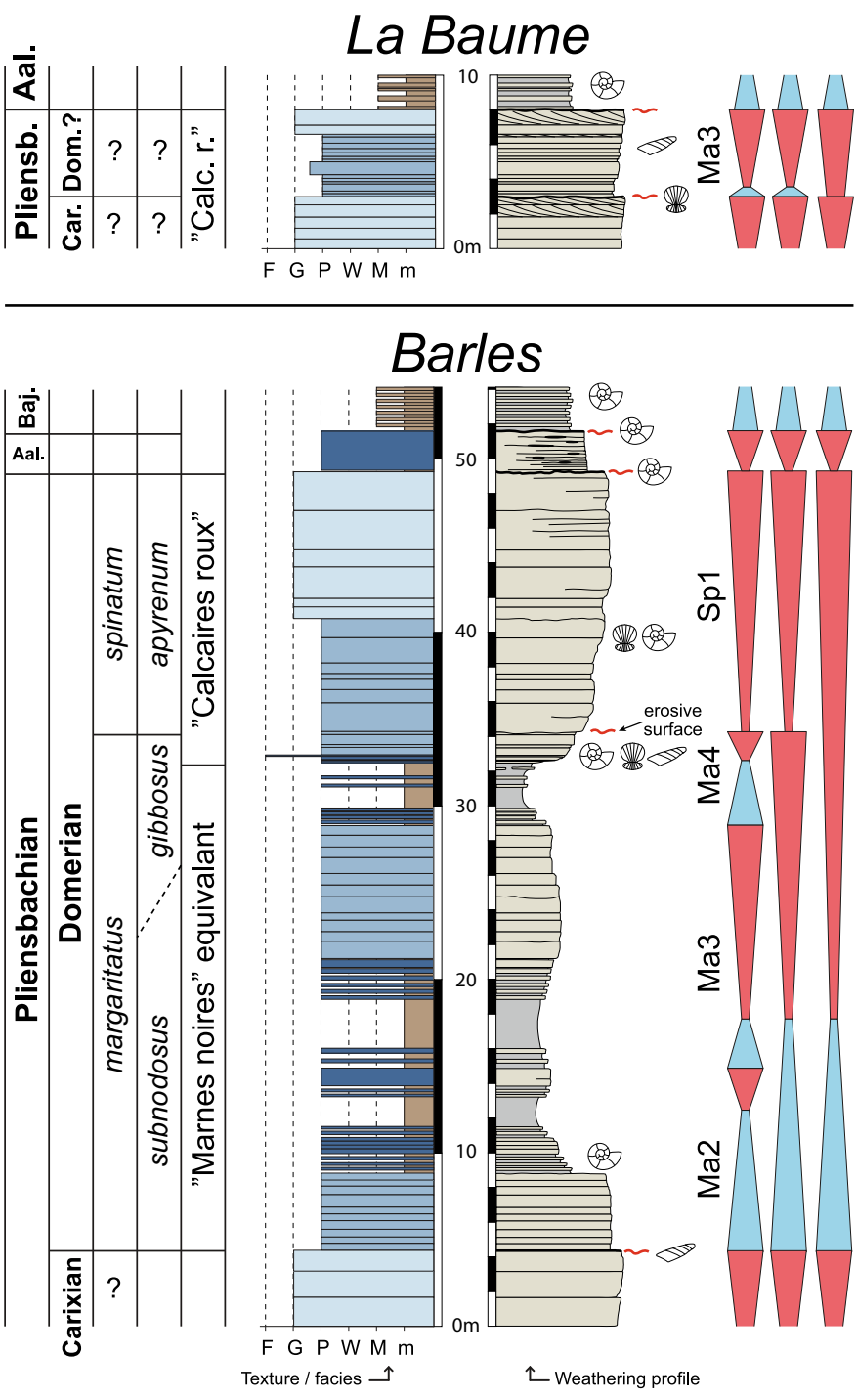

Fig. 2. Detailed log of La Baume and Barles sections, with carbonate texture and weathering profile evolution. Numerous hiatuses marked by ferromanganese crusts and hardgrounds are observed in these proximal sections. The transgressive/regressive trends are subdivided into short-, medium-, and long-term trends (refer to text for details). The key refers to facies color code, allochems, peculiar surfaces, and sequence stratigraphy. Abbreviations: Aal. – Aalenian; Car. – Carixian (lower Pliensbachian); Dom. – Domerian (upper Pliensbachian); "Calc. r." – "Calcaires roux"; Baj. – Bajocian.

geological map, the Pliensbachian is ca. 20 m thick (Kerckhove and Roux, 1976). Due to accessibility restriction, only the upper 8 m of the Pliensbachian have been logged in detail. The Barles section is situated along the hiking path on the western side of the Bès river, southwest of the Barles village (N44°15′41″, E6°15′57″; Fig. 2). The section covers the uppermost part of the Lower Pliensbachian to the lower Bajocian. The La Reine Jeanne section is situated ca. 2 km southeast of Digne-les-Bains. Its base is located next to the D20 road (N44°04′34″, E6°16′08″; Fig. 3) and was logged along the path leading to the "Chateau de la Reine Jeanne". The Rochebrune section is situated along the Bès river, on the northwestern side of a small hill known as "Champ Géran" (N44°0922″, E6°14′38″; Fig. 4). Only the upper Upper Pliensbachian is suitably exposed in the studied area. The Le Mousteiret section is situated next to the small road ("route des Guenis") leading to the Bléone river from Le Brusquet village (N44°0954″, E6°17′43″; Fig. 5).

3.1.2. *Central High Atlas Basin, Morocco*

A total of 25 sections situated in the Dades Valley were previously presented by Krencker et al. (2022) and Andrieu et al. (2022), forming a proximal to distal transect within the Central High Atlas Basin (Fig. 2). Within this transect, the Bou Oumardoul n'Imazighn composite section was first presented by Krencker et al. (2015) and Bodin et al. (2016), in which detailed sedimentological descriptions can be found. The section is situated in front of the toe-of-slope of the Pliensbachian Choucht carbonate platform (Krencker et al., 2022; Andrieu et al., 2022).

Biostratigraphic dating of the presented sections is based on

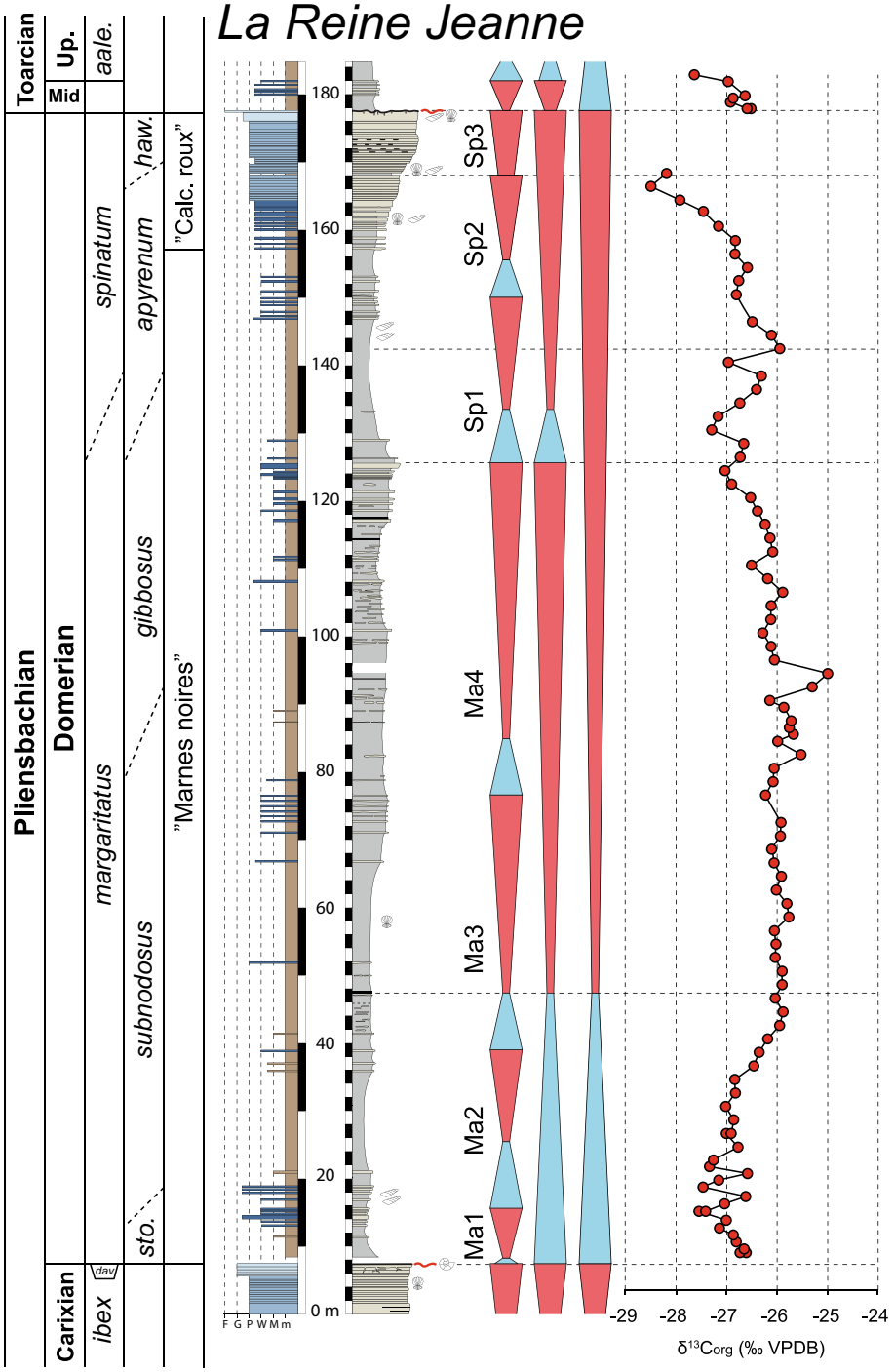

Fig. 3. Detailed log of La Reine Jeanne section, with corresponding bulk-rock $\delta^{13}C_{org}$ data. Dominance of ammonite and calcareous nannoplankton-bearing marls is observed in most of the Upper Pliensbachian (Domerian) indicating offshore depositional environments, except for the uppermost Pliensbachian where a substantial shallowing of facies toward nearshore depositional environments can be observed. For key to facies color code, allochems, and sequence stratigraphy, refer to Fig. 2. Abbreviations: aale. – aalensis; dav - davoei; Mid – Middle; Up. - Upper; sto. – stockesi; haw. – hawskerense; "Calc. roux" – "Calcaires roux".

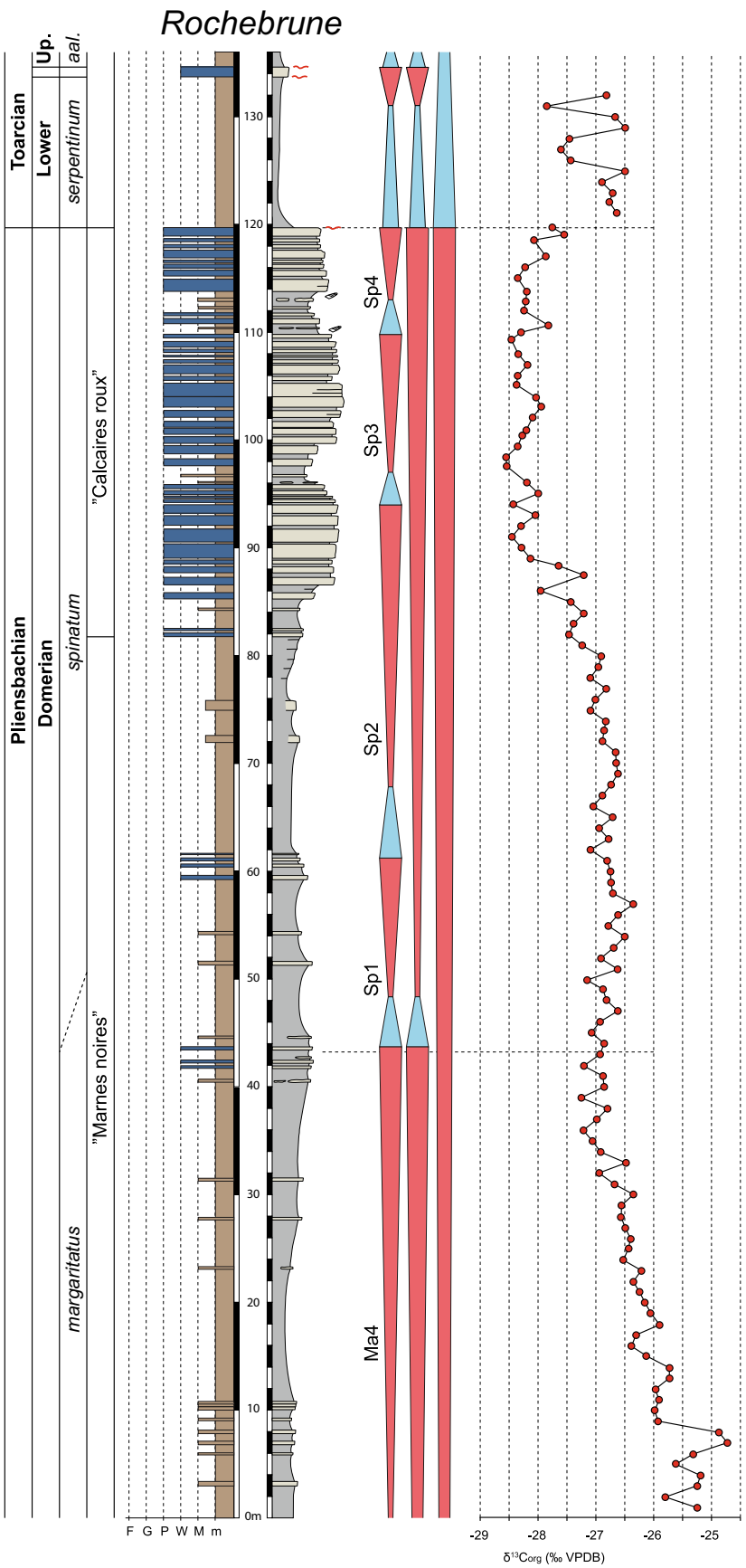

Fig. 4. Detailed log of the Rochebrune section, with corresponding bulk-rock $\delta^{13}C_{org}$ data. As in the La Reine Jeanne section, carbonate-rich facies are only present in the uppermost Pliensbachian. The facies are nonetheless more distal and remain within offshore environments. For key to facies color code, allochems, and sequence stratigraphy, refer to Fig. 2. Abbreviations: Up. - Upper; aal. – aalensis.

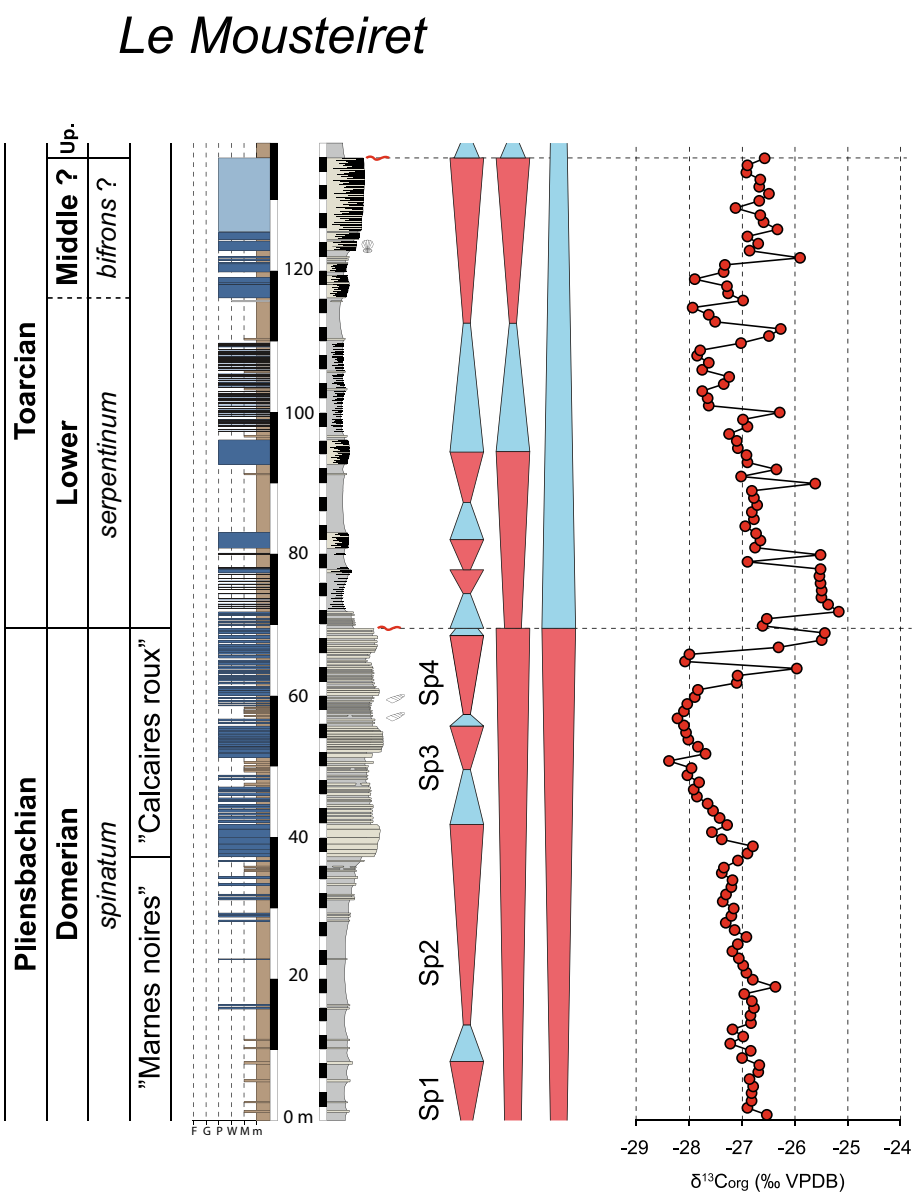

Fig. 5. Detailed log of Le Mousteiret section, with corresponding bulk-rock $\delta^{13}C_{org}$ data. A relatively expanded (ca. 65 m thick) lower – middle Toarcian is present in this section. The absence of a large negative $\delta^{13}C_{org}$ shift in the lower Toarcian confirms that the Toarcian OAE is not present in this section as also inferred from regional ammonite biostratigraphy. Most of the lower Toarcian is hence missing at the top of the Pliensbachian. For key to facies color code, allochems, and sequence stratigraphy, refer to Fig. 2. Abbreviations: Up. – Upper.

ammonite and brachiopod findings described in Ettaki et al. (2000), Ettaki and Chellai (2005), Krencker et al. (2015), and Bodin et al. (2016). Chronostratigraphic attribution is further strengthened by bulk organic carbon isotope chemostratigraphy (Bodin et al., 2016; Krencker et al., 2015, 2020, 2022).

3.2. Fieldwork, sampling, and facies analyses

In the South-East France Basin, the five studied sections were chosen for their accessibility and excellent exposure, allowing detailed and continuous lithostratigraphic observations, as well as the sampling of fresh unaltered material. Information about lithology, sedimentary textures and structures, as well as paleontological assemblages were made in the field. These observations were further complemented by the petrographic analysis of 24 thin sections. Both field and microscope observations were instrumental for the establishment of a facies model.

3.3. Organic carbon isotope analyses

Carbon isotope composition of bulk organic matter ($\delta^{13}C_{org}$, ‰, VPDB) were determined on 365 decarbonated powdered whole-rock samples (treatment with HCl, see Bodin et al., 2016) from La Reine Jeanne, Rochebrune, and Le Mousteiret sections. No carbon isotope analyses were performed on the La Baume and Barles sections owing to the absence of sufficient amount of organic matter in most part of these sections. The $\delta^{13}C_{org}$ values were measured using a Flash EA 2000 elemental analyzer connected online to ThermoFinnigan Delta V Plus mass spectrometer at the University of Erlangen-Nuremberg, Germany. Reproducibility was ±0.08‰.

3.4. Total organic content analyses

A total of 201 samples were analyzed for their total organic carbon content (TOC) in the Bou Oumardoul n'Imazighn composite section while measuring the $\delta^{13}C_{org}$ for the dataset presented in Bodin et al. (2016) (Morocco; Sections S8 and S11 in Krencker et al., 2022). The measurements were conducted using a Finnigan MAT 252 at the stable isotope laboratory of the Institute for Geology, Leibniz University Hannover (LUH), Germany. 2 g of sample powder were treated twice with 25 ml of 6 N HCl to remove the inorganic carbonate phase. Following centrifugation, the supernatant was removed. Residues were thoroughly rinsed several times with distilled water and finally dried at

60 °C. The TOC was determined using the positive correlation existing between the organic carbon weight and the Mass44 ion beam intensity (or peak area). The quality of the measurements was calibrated and controlled using LUH internal standards.

3.5. Mercury content analyses

Mercury (Hg) content analyses were performed on 272 samples from the Bou Oumardoul n'Imazighn composite section (Morocco; cf. Bodin et al., 2016) at the ISTE-UNIL of Lausanne (Switzerland) using a Zeeman R-915F (Lumex, St-Petersburg, Russia) high-frequency atomic absorption spectrometer set at Mode 1 (700 °C). Analyses were performed in duplicate on whole-rock powdered samples and calibrated using a certified external standard (GSD-11, Chinese alluvium; Hg: 72 ± 6 ppb; $r = 0.99$, for measured vs certified values) to guarantee the analytical quality. To distil out the potential influence of TOC content on Hg concentration, Hg/TOC ratios were also calculated (e.g., Sanei et al., 2012; Grasby et al., 2019).

3.6. Sequence stratigraphy

For each section in the South-East France Basin, the depositional sequences defined here are based upon the transgressive-regressive (T-R) sequence model of Embry and Johannessen (1992). Depositional sequences are hence interpretated using paleo-water-depth fluctuations as deduced from facies interpretation and the nature of their bounding surfaces (subaerial exposures, hardground, subaqueous erosion surface). We have hierarchized T-R sequences into three categories: long, medium and short-term sequences. The significance of facies shift, the extent to which the sequence boundary can be recognized throughout the South-East France Basin and the magnitude of the deepening/shallowing associated with the transgressive/regressive systems tracts are the fundamental criteria upon which this hierarchy is based on. At a basin scale, subdivision of the depositional sequence into a three-stage systems tract model (TST, HST, FSST/LST; cf. Catuneanu et al., 2011) is based upon the recognition of specific stratal stacking patterns along the here-defined proximal–distal transect in the South-East France Basin. The grouping of FSST and LST into one unified systems tract is due to the fact that they are ambiguous to differentiate in the transects here-studied.

4. Results and interpretations

4.1. Lithostratigraphy and biostratigraphy of the South-East France Basin

4.1.1. La Baume

The Pliensbachian of La Baume is made of crinoidal limestones with large-scale cross-stratification (Sup_Mat: Fig. S2a-b). It is capped by a ferromanganese crust showing stromatolitic structures (Sup_Mat: Fig. S2c), in which ammonites from the Toarcian *bifrons*, *thouarsense*, and *aalensis* zones have been found (Kerckhove and Roux, 1976). This crust is overlaid by hemipelagic limestone-marl alternations, out of which the first ca. 10 m are dated from the latest Aalenian (De Baets et al., 2008). This ferromanganese crust is thus associated with considerable condensation/hiatus. No specific biostratigraphic marker has been found in the Pliensbachian of this section. By lithostratigraphic comparison to regional geology, Kerckhove and Roux (1976) have nonetheless proposed that these crinoidal limestone belong to the Lower Pliensbachian. Another level of ferromanganese crust situated ca. 5 m below the top of the Pliensbachian (Fig. 2) has however been observed during our investigations. Hence by analogy to regional geology, we propose to correlate this lower peculiar surface to the regional hiatal surface associated with the top of the Lower Pliensbachian and therefore, the uppermost ferromanganese crust to the top of the Upper Pliensbachian (similar to the Barles and La Reine Jeanne sections, cf. below).

4.1.2. Barles

The top of the Lower Pliensbachian is made of coarse sand-sized crinoidal limestones, capped by a hardground surface with iron-oxide mineralization rich in belemnites. This is followed by a mixed quartz-rich limestone–black marl interval containing few brachiopods and bivalves. The base of the first back marl interval belongs to the *margaritatus* zone (*subnodosus* subzone), as indicated by the presence of *Amaltheus margaritatus* and *A. subnodosus* in this stratigraphic interval in a nearby section (Coadou et al., 1971) On top of the second black marl interval, at 33 m, a surface rich in ammonites, belemnites, bivalves, and phosphatic pebbles is observed, likely indicative of a condensed horizon. The presence of *Arieticeras* sp. and *Amaltheus margaritatus* (Coadou et al., 1971) indicates the *margaritatus* zone, *gibbosus* subzone. Coarse crinoidal limestones of the "calcaire roux" unit follow. At 34.4 m, a marked erosive surface is observed. Above this surface, the presence of *Pleuroceras solare* indicates the *spinatum* zone, *apyrenum* subzone (Coadou et al., 1971; Haccard et al., 1989). This unit is capped by a hardground surface, showing numerous borings and iron-oxide mineralizations, followed by a thin (few cm-thick) marl layer rich in ammonites from the uppermost Toarcian *aalensis* zone (Coadou et al., 1971). The next ca. 3 m are made of chert-rich crinoidal limestone, capped by a hardground surface dated from the *concavum* zone (late Aalenian; Coadou et al., 1971). An Aalenian age for this chert-rich crinoidal unit is therefore most likely. Finally, hemipelagic limestone-marl alternations dated at their base from the *humphriesianum* zone (middle Bajocian; Coadou et al., 1971) characterize the end of this section.

4.1.3. La Reine Jeanne

The uppermost lower Pliensbachian is made of coarse, sand-sized crinoidal limestone beds that contains fragments of bryozoan, brachiopods, and bivalves. A phosphate-rich hardground crust caps the lower Pliensbachian. It contains numerous ammonites (Haccard et al., 1989), indicating a condensed interval encompassing the late early Pliensbachian *davoei* zone to the lower *margaritatus* zone (*stokesi* subzone). This is followed by a thick interval dominated by black marls containing ammonites from the *margaritatus* zone (de Graciansky et al., 1982, 1993). At its base, the bioclastic limestone beds contain belemnites, bivalves, and few gastropods. In between ca. 70 m and 130 m, numerous limestone nodules and beds are intercalated in the black marls. Their occurrence and size increase toward the top of this interval, making a clear geomorphological break in the landscape. The interval from ca. 130 m to 145 m is characterized by the abrupt switch to a limestone-free lithological interval. In the upper part of the lateral equivalent of this interval in the nearby Marcoux section, de Graciansky et al. (1993) mention the presence of the ammonite *Pleuroceras solare*, indicative of the uppermost Pliensbachian *spinatum* zone, *apyrenum* subzone.

This interval is followed by ca. 20 m of crinoidal limestone of the "calcaire roux" unit, showing an overall coarsening-upward trend. In nearby sections, ammonite finds in the uppermost part of this unit are indicative the uppermost Pliensbachian *spinatum* zone, *hawskerense* subzone (de Graciansky et al., 1993). The top of this unit is marked by a rugged surface showing numerous bioturbation (firmground to hardground surface) with iron-rich mineralizations (Sup_Mat: Fig. S2). This surface is overlaid by 2 m of marl, dated from the early Toarcian, followed by ca. 2 m of bioclastic wackestones, dated from the middle Toarcian (Haccard et al., 1989), and uppermost Toarcian black marl from the *aalensis* zone, which can be up to 150 m thick in this area (de Graciansky et al., 1993).

4.1.4. Rochebrune

The Rochebrune section is situated along the Bès river, on the northwestern side of a small hill known as "Champ Géran" (N44°0922″, E6°14′38″; Fig. 4). Only the uppermost Pliensbachian is suitably exposed in the studied area. The first 82 m of this section is dominated by black marl, representing the uppermost part of a marl-dominated unit that locally reaches a total thickness of ca. 200 m (de Graciansky et al.,

1993). Within the logged part of this marl-dominated unit, two intervals with crinoidal wackestone beds occur around ca. 42 m and 60 m. No ammonite was found, but most of the upper Pliensbachian marls are usually assigned to the *margaritatus* zone in the literature (de Graciansky et al., 1993; Célini et al., 2020), although the position of the *margaritatus/spinatum* zonal boundary is not precisely known.

The "calcaire roux" unit is ca. 35 m thick and is made of alternating bioturbated crinoidal packstone and black marlstone beds. Two marl-rich intervals are observed within the "calcaire roux" unit at ca. 97 m and 103 m (Sup_Mat: Fig. S1). Several ammonites characteristic of the *spinatum* zone have been locally found in the uppermost bed of the "calcaire roux" unit (Floquet et al., 2003). The top of the upper Pliensbachian is characterized by a pyritized and fractured hardground surface, infilled by a bioclastic-rich packstone. In the nearby Marcoux section, one specimen of *Harpoceras serpentinum* was found within the fracture infill (Floquet et al., 2003). The upper Pliensbachian is overlaid by ca. 14 m of lower Toarcian black marls dated from the late *serpentinum* chronozone (Floquet et al., 2003). This is followed by a ca. 50 cm thick condensed carbonate bed dated from the middle Toarcian *bifrons* chronozone, overlaid by upper Toarcian black marls dated from the *aalensis* chronozone (Floquet et al., 2003). Most of the lower Toarcian and middle–upper Toarcian is therefore missing in this section.

4.1.5. Le Mousteiret

The studied uppermost Pliensbachian succession is 69 m thick. In its lower part, 37 m of black marl irregularly intercalated with mudstone and micro-packstone beds occur. The occurrence of fine grained (silt grain size) packstone beds (hereafter named micro-packstone) increases upsection. From the geological map (Haccard et al., 1989), it can be calculated that the overall thickness of the upper Pliensbachian marls is ca. 220 m. This is followed by a ca. 32 m-thick "calcaire roux" unit, made of alternating bioturbated crinoidal packstone and black marlstone beds. Two marl-rich intervals occur in this unit at around 50 m and 58 m in the section. The top of the "calcaire roux" unit is characterized by a sharp transition with the overlaying marl-dominated unit. Contrary to the other sections, no notable sedimentary or early diagenetic feature is observed on the surface marking the top of the "calcaire roux" unit in this section.

Black marl deposits with numerous intervals of finely layered marly micro-packstone follow the upper Pliensbachian. No ammonite was found in this section, but the same lithostratigraphic unit in the nearby Marcoux sections is dated from the early Toarcian (*serpentinum* zone; Floquet et al., 2003). This unit is overlaid by 20 m of layered micro-packstone that is regionally assigned to the middle Toarcian (Haccard et al., 1989). Its top is marked by a sharp transition to the upper Toarcian black marls (*pseudoradiosa* – *aalensis* zones; de Graciansky et al., 1993).

4.2. Sedimentary facies and depositional environments of the South-East France Basin

The crinoid-dominated Pliensbachian deposits in the South-East France Basin are similar to those described from the Pliensbachian of the nearby Southern Provence Sub-basin (Léonide et al., 2007). They are also reminiscent of those observed in the Toarcian of Italy (Monaco, 1992), the middle Jurassic of eastern France (Thiry-Bastien, 2002), or the lower Cretaceous of the NW Tethyan margin (Bodin et al., 2006; Gréselle and Pittet, 2010). According to their texture, grain size, sedimentary structure, and lithological and faunistic content, a total of 4 facies indicating 4 depositional environments can be distinguished (Fig. 6). These facies characterize a Heterozoan wave-dominated carbonate ramp.

4.2.1. Coarse crinoidal grainstone: upper shoreface deposits

Description: This facies is characterized by moderately sorted, fine to coarse crinoidal grainstone (Sup_Mat: Fig. S3a). It contains infrequent fragments of peloids, bivalves, sea urchin spines, gastropods, and bryozoans. Partial micritization of grains and microbialitic cement are occasionally observed. The beds are amalgamated together, display sharp erosional contacts, and are between 20 cm and 1 m thick. Large (50 cm thick, up to 5 m wide) seaward-directed trough cross-bedding is locally observed.

Paleoenvironmental interpretations: The presence of cross-stratified, amalgamated grainstone beds, and more specifically the absence of micrite, as well as the absence of any indication for tidal influence, suggests deposition in high-energy setting most likely above the fair-weather wave base (Thiry-Bastien, 2002), similar to upper shoreface deposits in wave-dominated siliciclastic settings (Clifton, 2006). The seaward-directed cross-bedding can therefore be assigned to bedforms formed by rip currents (Clifton, 2006).

4.2.2. Amalgamated crinoidal packstone: lower shoreface deposits

Description: This facies is characterized by packstone made of moderately to poorly sorted, medium crinoidal sand (Sup_Mat: Fig. S3b). Frequent peloids, as well as fragments of bivalves, brachiopods, gastropods, sea urchin spikes and shells, serpulids, and infrequent benthic foraminifera and bryozoans fragments are also present. Quartz grains are also infrequently observed. The beds are undulatory, and between 10 and 60 cm thick, display sharp erosional contacts, and are amalgamated together. Faint cross-stratifications are also occasionally observed.

Paleoenvironmental interpretations: The undulatory character of the

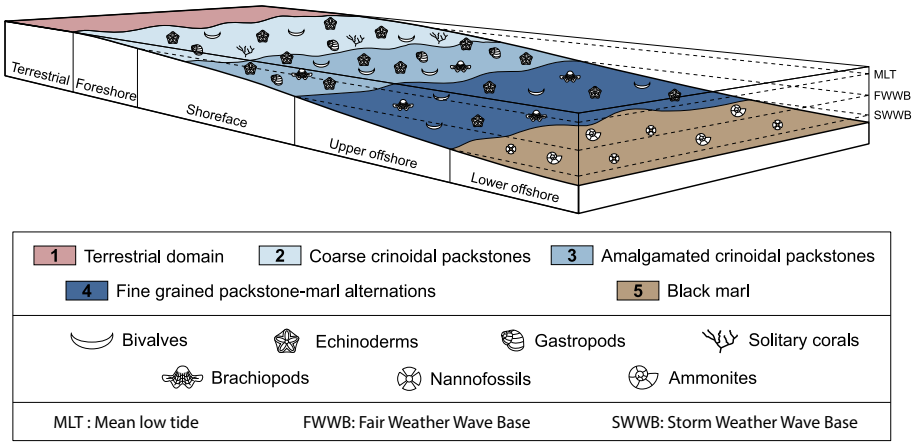

Fig. 6. Block diagrams showing depositional environments and key palaeontologic elements for the Pliensbachian carbonate ramp in the SE France Basin. Bioclastic carbonate, dominated by crinoids, were produced in nearshore environments and exported in offshore environments during storms. This sedimentary system is thus relatively similar to a wave-dominated siliciclastic shelf.

beds and their sharp erosional contacts are reminiscent of carbonate beds deposited by storm waves (e.g., Krencker et al., 2020). Together with the absence of marl interbeds, this indicates deposition above the fair-weather wave base, likely in the lower shoreface by analogy to wave-dominated siliciclastic settings (Clifton, 2006).

4.2.3. Fine grained packstone-marl alternations: upper offshore deposits

Description: The rocks belonging to this depositional environment are characterized by limestone-marl alternations. The limestone beds are 10 to 50 cm thick and made of very fine to fine grained laminated packstone, mainly composed of echinoderms and bivalve fragments, plus other unidentified bioclasts, as well as infrequent quartz grains (Sup_Mat: Fig. S3c). Occasionally, monoaxial sponge spicules are observed. Sponge spicules and calcareous nannofossils are also present in the marls, which are otherwise devoid of shallow-marine benthic allochems. Belemnites are occasionally found. The base of the limestone beds is sharp, whereas a more diffuse transition to the marl beds is often observed at their top.

Paleoenvironmental interpretations: An offshore marine environment can be inferred from the presence of belemnites and calcareous nannofossils. The alternation of packstone beds with marl interlayers suggest intermittent deposits of reworked nearshore sediments under wave action in an otherwise calm environment. This is typical of storm deposits in upper offshore settings (Clifton, 2006).

4.2.4. Black marl: lower offshore deposits

Description: This facies is mostly made of thick grey to black marls containing calcareous nannofossils and infrequent sponge spicules (Sup_Mat: Fig. S3d), as well as rare ammonites and belemnites. Occasionally, mudstone beds are present within the marls. The mudstone beds are often discontinuous, giving them a nodulous aspect. Rare occurrence of thin very fine grained packstone beds is also observed.

Paleoenvironmental interpretations: The presence of ammonites, belemnites, and calcareous nannoplankton suggest an offshore marine environment. Marls and mudstones are indicating deposition by suspension settling below the storm wave base, in lower offshore settings. The very fine grained packstone beds can be related to materiel shed off from shallower setting during exceptional storm events.

4.3. Carbon isotope chemostratigraphy of the South-East France Basin

The $\delta^{13}C_{org}$ curve of the Reine Jeanne section shows that the *margaritatus* zone is characterized by a large positive $\delta^{13}C_{org}$ excursion reaching a climax in the upper part of the zone, followed by a long-term negative excursion toward the top of the *spinatum* zone. The $\delta^{13}C_{org}$ curves from Rochebrune and Le Mousteiret show a similar long-term trend, from relatively high values in the *margaritatus* zone toward relatively lower values in the *spinatum* zone (Fig. 7). This long-term trend is similarly observed in numerous other basins in both carbonate and organic matter $\delta^{13}C$ values (e.g., Valencio et al., 2005; Oliveira et al., 2006; Rosales et al., 2006; Suan et al., 2010; Korte and Hesselbo, 2011; Peti et al., 2017; De Lena et al., 2019; Storm et al., 2020; Schöllhorn et al., 2020; Franceschi et al., 2022), highlighting the reliability of the $\delta^{13}C_{org}$ record in the South-East France Basin for intra- and inter-basinal chemostratigraphic correlation.

Within the overall fall of $\delta^{13}C_{org}$ after the climax of the *margaritatus* zone, a short-lived $\delta^{13}C_{org}$ positive excursion is also observed around the

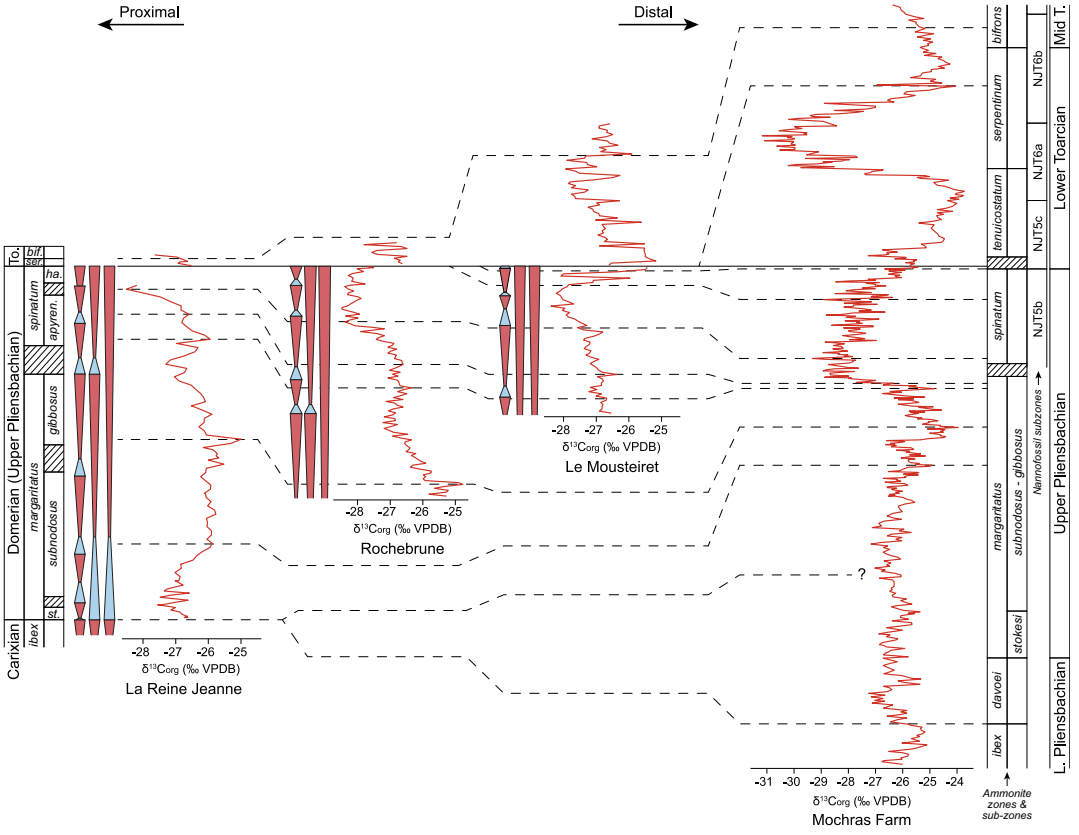

Fig. 7. Correlation of the $\delta^{13}C_{org}$ records in the SE France Basin with the reference Mochras Core record (Xu et al., 2018; Storm et al., 2020). This correlation emphasizes the increasing completeness of the top Spinatum chronozone with increasing distance toward the basin centre. The position of the Pliensbachian/Toarcian boundary in the Mochras core is based on the first occurrence of the nannofossil *Zeugrhabdothus erectus* (base of NJT5c zone; Menini et al., 2021) rather than on ammonite biostratigraphy due to the presence of a 4.67 m ammonite-barren interval below the first occurrence of *Dactylioceras* ammonites in this core (Ivimey-Cook, 1971). See text for discussion. Abbreviations: To. – Toarcian; ser. – serpentinum; bif. – bifrons; st. – stockesi; ha. – hawskerense;

margaritatus–spinatum zones transition in the three sections. A similar behaviour is seen in the high-resolution record of the Mochras core in Wales (Storm et al., 2020), although this latter is reported within the uppermost *margaritatus* zone. This slight difference in biostratigraphic allocation could either be linked to imprecise biostratigraphic record in either French sections or the Mochras core. Alternatively, minor lag in the first appearance datum of ammonites characteristic of the *spinatum* zone between the Boreal and the Tethyan realms could also be evoked.

Significant differences in $\delta^{13}C_{org}$ trends appear in the upper *spinatum* zone between the three studied sections. At La Reine Jeanne section, a negative $\delta^{13}C_{org}$ shift is recorded, whereas at Rochebrune this negative trend is followed by a plateau of negative values, and at Le Mousteiret, a positive shift follows the negative plateau of $\delta^{13}C_{org}$ values in the uppermost part of the *spinatum* zone. These differences in the $\delta^{13}C_{org}$ trends within the South-East France Basin are attributed to condensation levels or incompleteness of the sedimentary record. This interpretation is based on the presence of clearly documented hiatuses or condensation at the top of the *spinatum* zone within the basin, and on the chemostratigraphic correlation to the reference record of the Mochras core in Wales (Storm et al., 2020) showing that the Spinatum chronozone is characterized by a large negative carbon isotope excursion followed by recovery to pre-excursion values in its uppermost part. In Fig. 7, the chemostratigraphic correlation between the three studied sections from France and the Mochras core highlights that the completeness of the *spinatum* zone is related to the position of the section within the basins, with completeness increasing toward the basin centre.

Finally, in the three newly analyzed sections, the Toarcian $\delta^{13}C_{org}$ record clearly shows the absence of any large negative carbon isotope excursion that could be attributed to the T-OAE, confirming that only the upper part of the *serpentinum* zone is preserved in this area (cf. Floquet et al., 2003; Léonide et al., 2012).

4.4. Total organic matter and mercury content in the Bou Oumardoul n'Imazighn section

In the limestone-marl alternations of the Pliensbachian, the TOC content fluctuates around 0.75% (Fig. 8). This is followed by a marked decrease to values around 0.2% in the siliciclastic Tagoudite Formation (lowermost Toarcian). In the overlaying Tafraout and Azilal Formations (upper lower Toarcian – upper Toarcian), the TOC values show an overall background value centred around 0.3% with few horizons showing values above 0.5%. In the lowermost part of the Tafraout Formation (upper *polymorphum* zone), a significant interval of high TOC values is observed, with values reaching up to 2.4%. This interval corresponds to black lagoonal shale deposits rich in continental organic matter (cf. Bodin et al., 2016; Brame et al., 2019) and is coeval to a small positive $\delta^{13}C_{org}$ excursion.

The Hg content (Fig. 8) shows an overall background level of ca. 5 ppb, punctuated by 3 intervals of significant enrichment that can be observed in more than two consecutive samples. The first interval is centred around the Pl/To boundary, with values reaching up to ca. 20 ppb. A second interval of similar Hg enrichment occurs in the lowermost part of the Tafraout Formation and is associated to the lagoonal black shales previously described. The third enrichment interval, with Hg concentration values reaching ca. 30 ppb, covers the lower 2/3 of the T-OAE interval as defined by the ca. 5‰ negative $\delta^{13}C_{org}$ excursion in this section (cf. Bodin et al., 2016).

In the T-OAE interval, Hg anomalies are mirrored by Hg/TOC values,

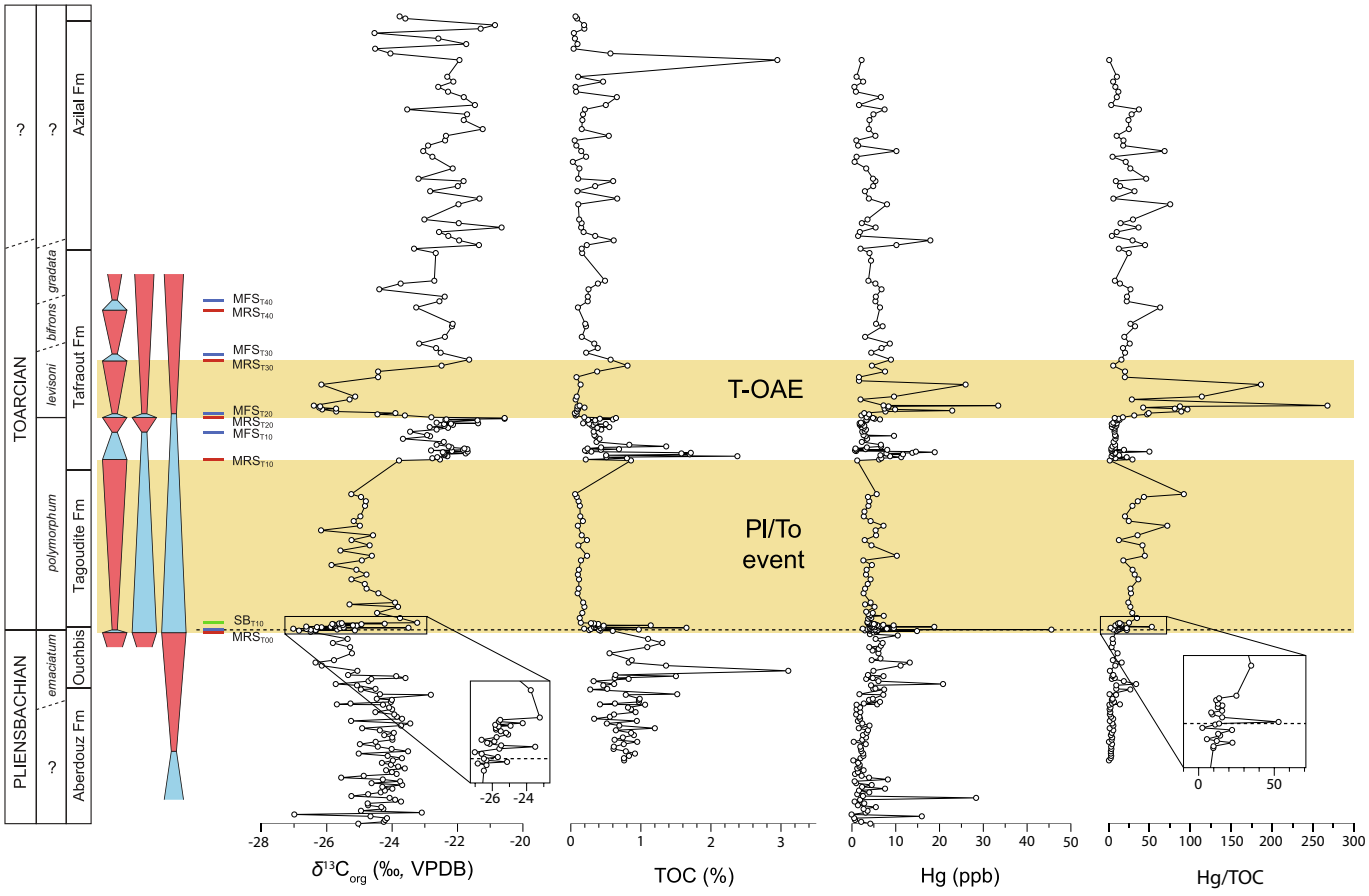

Fig. 8. Sedimentary mercury [Hg], TOC, and Hg/TOC record of the Bou Oumardoul n'Imazighn section (Central High Atlas Basin, Morocco) showing elevated [Hg] in the T-OAE interval and at the onset and termination of the Pl/To event interval. See text for discussion. Biostratigraphy and bulk-rock $\delta^{13}C_{org}$ data are from Bodin et al. (2016). Sequence stratigraphy interpretation is from Krencker et al. (2022). The dashed line indicates the position of the Pliensbachian/Toarcian boundary.

supporting a genuine increase of Hg content in the environment. In contrast, Hg anomalies associated with Hg/TOC close to background values recorded at the Pl/To boundary and in the lower Tafraout Formation indicate that Hg is primarily linked to increased organic matter content in the sedimentary rocks of the the Bou Oumardoul n'Imazighn section (Fig. 8).

5. Sequence stratigraphy of the South-East France Basin

5.1. Transgressive – regressive cycles and proximal – distal correlation

According to facies stacking patterns and key surfaces marking non-Waltherian facies changes and/or condensed horizons, three orders of transgressive – regressive (T-R) trends can be identified in most of the sections (Figs. 2–5 and Fig. 9). The top of the lower Pliensbachian marks the end of a long-term regression recognized regionally (de Graciansky et al., 1993). The upper Pliensbachian is recording one long-term asymmetric T-R sequence with a maximum flooding surface (MFS) situated within the *margaritatus* zone (*subnodosus* subzone). Its lower and upper boundary (maximum regressive surface; MRS) are the two regional unconformities well recognisable by the presence of hardground and phosphatic crust/nodules, and by biostratigraphic hiatus. The Upper Pliensbachian long-term cycle can be subdivided into two medium-term sequences; a first one spanning the *margaritatus* zone, and a second one spanning the *spinatum* zone. The MFS of the first medium-term sequence is the same as the Upper Pliensbachian long-term cycle MFS, whereas the MFS of the second medium-term sequence is situated in the lower part of the *spinatum* zone (*apyrenum* subzone). In the more distal sections (Reine Jeanne, Rochebrune, Le Mousteiret), the MRS separating these two medium-term sequences is placed on top of the more carbonate-rich beds belonging to the uppermost *margaritatus* zone and preceding a marked facies-deepening trend in the lowermost part of the *spinatum* zone. In the Barles section, the MRS corresponds to the erosive base of a 1 m thick bed within the lowermost part of the "Calcaires roux" unit. These long- and medium-term sequences are consistent with the sequence stratigraphy interpretation of de Graciansky et al. (1993). They have an asymmetric stratigraphic character, implying relatively fast and/or condensed transgression period/record, followed by a relatively long and/expanded progradation period/record.

The number of short-term sequences within the Upper Pliensbachian differs in between all the studied sections (Fig. 9). In the La Baume section, only one short-term cycle (Ma3) is recorded between the two iron-rich hardground surfaces delimiting the here-interpreted Upper Pliensbachian. In the Barles sections, 4 short-term sequences are present; 3 in the *margaritatus* zone (Ma2, Ma3, Ma4), and a last one in the *spinatum* zone (Sp1). In the Reine Jeanne section, 4 sequences are recognized in the *margaritatus* zone (Ma1, Ma2, Ma3, Ma4) and 3 in the *spinatum* zone (Sp1, Sp2, Sp3). The Upper Pliensbachian of the Rochebrune and Le Mousteiret was not logged in its entirety. Nevertheless, one complete sequence can be recognized in the uppermost part of the *margaritatus* zone in the Rochebrune section (Ma4), followed by 4 sequences in the *spinatum* zone (Sp1, Sp2, Sp3, Sp4). In the Le Mousteiret section, 3 complete sequences can be recognized in the *spinatum* zone (Sp2, Sp3, Sp4). The basal part of this section shows the upper regressive part of an initial sequence (Sp1), whereas the top of the *spinatum* zone records the beginning of a transgressive trend (Sp5) interrupted by the major unconformity of the Pliensbachian/Toarcian boundary. Overall, taking into account that the *spinatum* zone was not completely covered by our survey in the two most distal sections, a marked increase in the number of short-term sequences can be recognized along the proximal-distal transect represented by these sections.

Given that the vast majority of these Upper Pliensbachian short-term sequences are inscribed within a long-term regressive trend, this difference in the number of short-term sequences is best explained by a progradational stacking pattern (Fig. 9). This implies that in the most proximal sections, a significant amount of the Spinatum chronozone is missing at the top of the Upper Pliensbachian. The more proximal the section is, the more time is missing. Of particular importance here is that this sequence stratigraphy interpretation is fully consistent with the $\delta^{13}C$ chemostratigraphic correlation that suggests a similar pattern (Fig. 7). At least 4 complete short-term sequences characterize the *spinatum* zone in the SE France Basin, in addition to an incomplete one at the top of this zone represented by the lower part of a transgression trend.

Interestingly, based on the chemostratigraphic correlation between the South-East France sections and the Mochras core (see

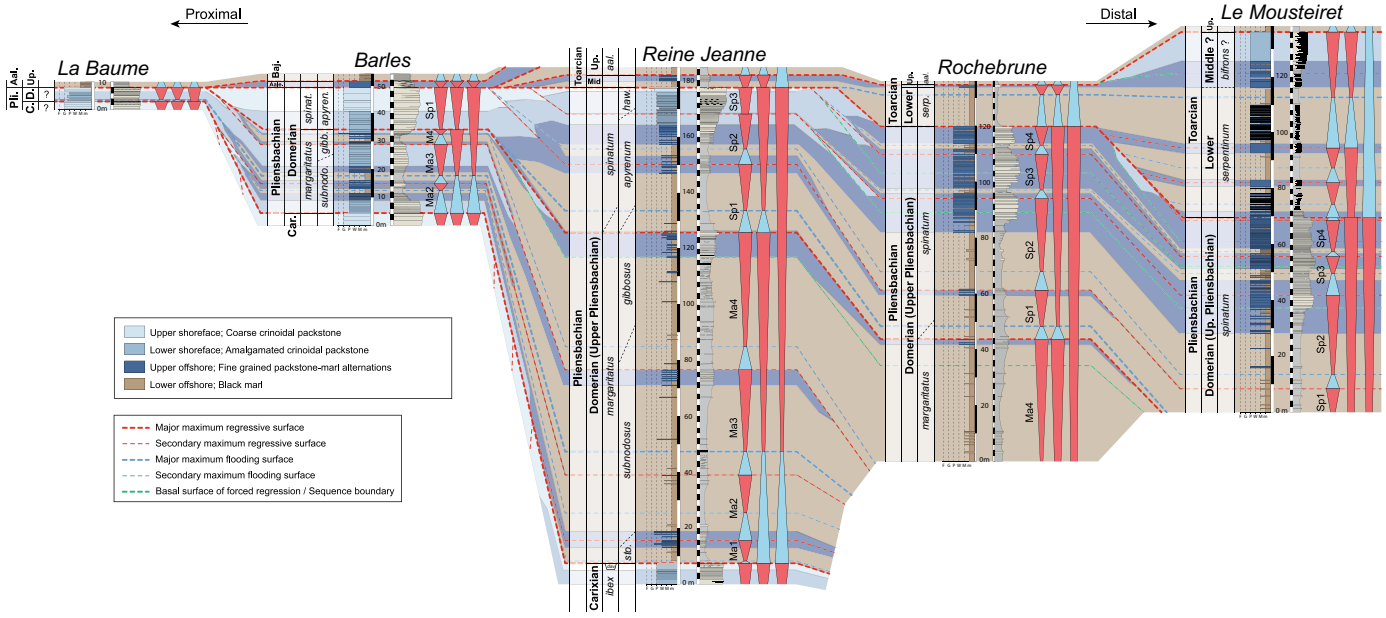

Fig. 9. Palinspastic correlation panel through the sections measured in the SE France Basin, arranged approximately perpendicular to the regional shoreline trend. The correlation is based on integrated biostratigraphy, carbon isotope chemostratigraphy (cf. Fig. 7), and T/R trends. This panel illustrates the facies partitioning and sequences relationship along a proximal–distal transect, highlighting the progressive pinch out of bioclastic clinoforms into offshore marls, as well as the strong progradation character of the uppermost Pliensbachian "calcaires roux" unit.

cyclostratigraphy study in Ruhl et al., 2016), a duration of ca. 1.7 Myr can be inferred for the medium-term sequence in the spinatum zone. Assuming an equal duration of the short-term sequences, and acknowledging that an incomplete 5th one is occurring at the top of the Upper Pliensbachian, an average duration in the order of the long eccentricity cycle (i.e., 405 kyr) can be deduced for these short-term sequences. This suggests that they could be driven by Milankovitch forcing, and possibly the waxing/waning of continental ice during one of the coldest time intervals of the Jurassic (Rosales et al., 2004; Suan et al., 2010; Korte and Hesselbo, 2011; Ruebsam et al., 2019).

The cross-section along the proximal–distal transect in the South-East France Basin (Fig. 9) illustrates the general progradation during the latest Pliensbachian and the diachronic onset of the "calcaire roux" unit. The presence of a short-term Late Regressive systems tracts (i.e., Falling Stage and Lowstand systems tracts) is suspected in distal sections for the last sequence of the *margaritatus* zone (Ma4) due to the presence of an erosive surface marking the *margaritatus/spinatum* zones boundary in the more proximal section of Barles. This later surface corresponds thus to a basal surface of forced regression (BSFR). Based on the presence of thick beds bundles in the upper part of the Sp2 and Sp3 sequences in the Rochebrune and Le Moustereit sections, the presence of Late Regressive systems tracts is also interpreted for these sequences, although firm evidence for short-term hiatuses in more proximal section could not be established. Finally, in the upper part of the last sequence of the *spinatum* zone (Sp4 sequence) in the Le Mousteiret section, the presence of a late regressive systems tract is also interpreted to explain the occurrence of the positive $\delta^{13}C$ shift at the top of the Upper Pliensbachian in this section (Fig. 7), which is otherwise absent in the more proximal Rochebrune section.

5.2. Supra-regional correlations

The correlation of sequence stratigraphy frameworks across several basins is intrinsically limited by available literature and the precision of the sequence stratigraphy approach in each basin, which is itself limited by the number of available sections/cores and the precision of their chronostratigraphic constraints. Given that fluctuation of relative sea-level can only be confidently assessed in shallow-marine records, sedimentary records from terrestrial or deep-marine environments are also inadequate for this endeavour, limiting de facto the number of available studies. Moreover, the exact chronostratigraphic position of MRS and MFS can also slightly vary in between each basin, due to either imprecision in chronostratigraphic attribution, or difference in regional subsidence and/or sedimentation rates which can induce heterochronicity in the timing of the transgression (Csato and Catuneanu, 2012; Krencker et al., 2022). Given all these limitations, it is nevertheless remarkable to note that the sequence stratigraphy pattern inferred in the South-East France Basin can be correlated to other basins from which detailed sequence stratigraphic studies are also available. This indicate that eustatic sea-level fluctuations were likely the main driver of these sequences deposition despite different subsidence and sediment supply history specific to each basin.

In numerous localities, the upper Pliensbachian is associated with a long-term T-R cycle with a MFS situated within the *margaritatus* zone. This is documented in both northern and southern hemisphere (Legarreta and Uliana, 1996; Pieńkowski et al., 2008; and reference therein). Unambiguous evidence for subaerial exposure on top of the Pliensbachian is also documented in numerous regions, such as in Italy (Carbone, 1984), Poland (Pienkowski, 2004), and Morocco (Merino-Tomé et al., 2012; Krencker et al., 2022). Interestingly, this long-term cycle coincides with a well-marked swing of seawater temperature, with peak temperature reached during the Margaritatus chronozone, followed by a long-term cooling toward the Spinatum chronozone (Rosales et al., 2004; Suan et al., 2010; Korte and Hesselbo, 2011; Baghli et al., 2020). A climate-driven eustatic sea-level cycle is hence likely at the origin of this long-term global T-R sequence.

Two upper Pliensbachian medium-scale sequences are also observed in the high-resolution studies from the British Isles (Howard, 1985; Hesselbo and Jenkyns, 1998), Poland (Pienkowski, 2004), SW France (Brunel et al., 1999). They can also be inferred from the northern Spain record (Quesada et al., 2005), although not explicitly reported due to the longer time scale resolution focus of this study. One medium-scale sequence is also observed in the *margaritatus* zone (*subnodosus* and *gibbosus* subzones) of Portugal (Silva et al., 2015). Unfortunately, this latter study did not make a sequence stratigraphy investigation of the *spinatum* zone in this basin. In NE France, Germany, and Denmark (Pieńkowski et al., 2008; and reference therein), these two medium-scale sequences are however not reported, but it should be noted that in these regions, only a subdivision at the long-term scale can be achieved due to the relatively deep depositional environment of the studied sections/cores during most of the upper Pliensbachian. In Poland, the MRS at the top of the *margaritatus* zone sequence is marked by the occurrence of continental deposits over a large portion of the polish basin (Pienkowski, 2004), implying a substantial fall of relative sea-level. No direct evidence for subaerial exposure has been observed in South-East France, but a hiatus spanning the upper *margaritatus* zone (*gibbosus* subzone) is generally often reported in France (Enay et al., 1980), which could be an indirect indication for shallowing and/or subaerial exposure over large part of the French basins. A similar erosion surface and hiatus is also reported from the Cleveland Basin (England; Howard, 1985; see also McArthur et al., 2000). The widespread distribution of these two medium-term sequences suggests that their formation was also driven by eustatic sea-level fluctuations.

The short-term sequences observed in South-East France can only be compared to the sequence stratigraphic frameworks from Poland and Great Britain, where similar high-resolution studies are also available. In the Cleveland Basin, 3 short-term sequences are reported in the *margaritatus* zone by Hesselbo and Jenkyns (1998), but this is mostly based on the Hawsker Bottom section, whereas regional correlations suggest the existence of at least 5 short-term sequences (Howard, 1985). Additionally, one short-term sequence is reported in the *spinatum* zone by Hesselbo and Jenkyns (1998). In the precise lithological column of the Robin Hood's Bay section (Hesselbo and Jenkyns, 1995), a first subordinate shallowing of facies can nevertheless be observed in the middle part of the *apyrenum* subzone (Fig. 10). Two complete short-term sequences in the *spinatum* zone could thus be inferred from this region. In Poland, 4 short-term sequences are reported in the *margaritatus* zone (sequence VI in Pieńkowski et al., 2020), and 2 in the following sequence VII spanning the *spinatum* zone (Pieńkowski et al., 2020). The number of short-term sequences is therefore remarkably similar in the *margaritatus* zone in these three basins, but variable in the *spinatum* zone. As highlighted by the SE France transect, this can be linked to the long-term sequence development of the upper Pliensbachian, with relatively large amount of accommodation space creation during the transgression and early regression stage of the *margaritatus* zone, followed by relatively low accommodation space creation during the late regression stage of the *spinatum* zone, inducing significant progradation of the shoreline. Importantly, this suggests that a hiatus is present at the top of the Pliensbachian in both British and Polish records.

6. Discussion

6.1. A negative carbon isotope excursion spanning the Pliensbachian/Toarcian boundary?

A negative $\delta^{13}C$ excursion, reaching a nadir in the lowermost Toarcian, was first observed by Hesselbo et al. (2007) from the bulk carbonate record of the Peniche section. The validity of this excursion as a chemostratigraphic marker for the base of the Toarcian was confirmed by the work of Littler et al. (2010) who highlighted the occurrence of a negative carbon isotope excursion spanning the Pl/To transition in the bulk organic matter of Hawsker Bottom section. Since this study,

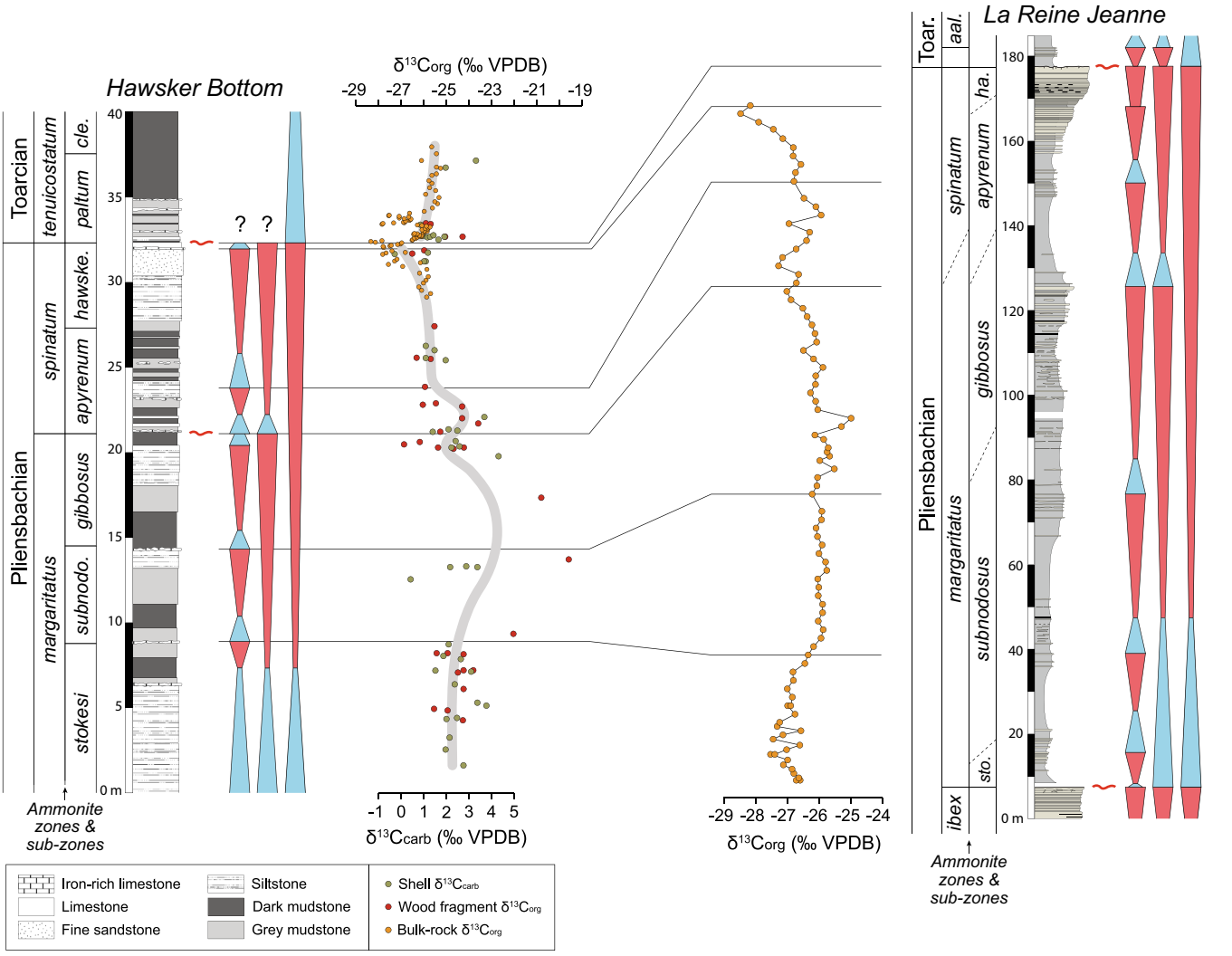

Fig. 10. Chemo-sequence stratigraphy correlation between the Hawsker Bottom (Cleveland Basin, UK) and La Reine Jeanne (SE France Basin) sections. The Hawsker Bottom section is redrawn after Hesselbo and Jenkyns (1995). C-isotope data are from Littler et al. (2010) and Korte and Hesselbo (2011). In the *spinatum* zone, the presence of a similar number of short-term sequences between the two sections as well as the absence of a complete negative C-isotope excursion (cf. correlation to data from Mochras core; Storm et al., 2020; Fig. 7) indicate that the top of the Spinatum chronozone is similarly missing in these two sections.

numerous studies have based their chronostratigraphic attribution on this chemostratigraphic feature to identify the Pl/To boundary (e.g., Ruebsam and Al-Husseini, 2020, and references therein). By analogy to the negative $\delta^{13}C$ excursion of the T-OAE, release of ^{13}C-depleted greenhouse gas inducing global warming was posited to explain the negative $\delta^{13}C$ excursion and by extension, the Pl/To event (Littler et al., 2010). However, the absence of the negative carbon isotope excursion spanning the Pl/To boundary in the high-resolution organic carbon isotope records from other biostratigraphically well-constrained sections such as in Morocco (Bodin et al., 2016), Chile (Fantasia et al., 2018), the Mochras core (Storm et al., 2020), or Argentina (Al-Suwaidi et al., 2022) have recently challenged the widely used assumption of a ubiquitous $\delta^{13}C$ negative trend starting in the latest Pliensbachian, reaching a nadir at the Pl/To boundary, and followed by a return to pre-excursion values immediately after. In these sections, instead of a negative trend, a positive trend of δ^{13}Corg values is recorded across the Pl/To boundary, thereafter followed by a negative excursion in the lowermost Toarcian (lower *tenuicostatum* zone). This discrepancy questions thus our understanding of the carbon cycle change across the Pl/To boundary and the reliability of some of the published isotopic curves as a global carbon cycle tracer.

A first important point is the fact that for sites where both carbonate ($\delta^{13}C_{carb}$) and organic ($\delta^{13}C_{org}$) carbon isotope records are available, different trends across the Pl/To transition are systematically observed (Bodin et al., 2016; Fantasia et al., 2019; Schöllhorn et al., 2020; Ullmann et al., 2022). Several studies have highlighted that carbon isotope values from bulk carbonates are less reliable as a tracer of global carbon cycle change during the Jurassic due to the absence of a significant pelagic carbonate factory as well as diagenetic overprinting (Bodin et al., 2016; Ullmann et al., 2022; Fantasia et al., 2022). This is linked to the fact that carbonate produced by neritic organisms in platform settings have higher $\delta^{13}C$ values than those produced by pelagic organisms (Swart and Eberli, 2005; Godet et al., 2006). There is thus a positive correlation between the relative amount of platform-derived carbonate in offshore deposits and their bulk carbonate $\delta^{13}C_{carb}$ value. Additionally, remineralization of organic matter will also create ^{13}C-depleted carbonate that might significantly lower $\delta^{13}C_{carb}$ values in carbonate-poor rocks (e.g., Bodin et al., 2016; Wohlwend et al., 2016). Hence, $\delta^{13}C_{carb}$ trends can be significantly influenced by change in carbonate content that can override interpretations of the carbon cycle dynamics. This can for example be observed in the high-resolution $\delta^{13}C_{carb}$ record of the Pl/To transition in the Peniche section where short-term, 1‰ oscillations of the $\delta^{13}C_{carb}$ are in phase with carbonate content fluctuations (Hesselbo et al., 2007). Given the collapse of both neritic and

pelagic carbonate production associated with the Pl/To event, it is thus not surprising to see in carbonate-dominated settings (e.g., Portugal, Morocco, Cardigan Bay) a negative $\delta^{13}C_{carb}$ excursion spanning the Pl/To transition but which is not faithfully reproducing the shape of the $\delta^{13}C_{org}$ curve (e.g., Bodin et al., 2006; Fantasia et al., 2018, 2019; Ullmann et al., 2022). This latter type of record can also suffer from potential biases, as $\delta^{13}C_{org}$ is influenced by organisms' growth rate, atmospheric pCO_2 changes, and other environmental factors (e.g., Hayes et al., 1999; Gröcke, 2002), as well as subject to potential pitfalls linked to mixing of different type of organic matter (Suan et al., 2015), but this latter can be easily assessed using Rock-Eval pyrolysis or palynological analyses. Overall, Jurassic $\delta^{13}C_{org}$ records appear nevertheless more robust than $\delta^{13}C_{carb}$ records to depict global change in the exogenic carbon cycle. These latter records show that the Pl/To boundary is characterized by a positive $\delta^{13}C$ trend, associated with the recovery part of the Spinatum chronozone negative carbon isotope excursion.

The inconsistency between the $\delta^{13}C_{org}$ record from the Yorkshire coast and those from Morocco, Wales, Chile, Argentina, and France can be resolved when applying a coupled chemo-sequence stratigraphy approach, allowing an improved chronostratigraphic precision beyond the resolution achieved by the sole ammonite biostratigraphy. Hence, in the Hawsker Bottoms section, the *spinatum* zone is 10 m-thick (Hesselbo and Jenkyns, 1995), out of which the upper third encompasses the negative $\delta^{13}C$ shift forming the lower part of Littler et al. (2010)'s Pl/To negative excursion (Fig. 10). This negative $\delta^{13}C$ shift is however the continuation of a longer-term negative trend initiated in the upper *margaritatus* zone as recorded in fossil shells and wood fragments (Korte and Hesselbo, 2011). When compared to other records, the negative trend in the *spinatum* zone of the Hawsker Bottoms section is thus best correlated to the negative shift of $\delta^{13}C$ values that covers the *margaritatus/spinatum* zones transition (Fig. 7), e.g., in the Mochras core (Storm et al., 2020), the Sancerre core (Peti et al., 2017), or the Breggia section (Schöllhorn et al., 2020). In fact, the Hawsker Bottom record is very similar to the Reine Jeanne record, where the *spinatum* zone is only recording a negative $\delta^{13}C_{org}$ shift initiated in the uppermost *margaritatus* zone. From a sequence stratigraphy point-of-view, there are also numerous similarities between the Hawsker Bottom and the Reine Jeanne sections. In particular, at both sites, only two short-term sequences encompass the stratigraphic interval covered by this negative $\delta^{13}C_{org}$ shift (Fig. 10). This suggest that only the two first short-term sequences of the Spinatum chronozone are present in the Hawsker Bottom section.

Altogether, these observations reinforce the interpretation that the uppermost Spinatum chronozone is missing in the Hawker Bottom section. As already suggested by Morard et al. (2003), this hiatus explains the absence of the *elisa* subzone (upper *hawskerense* zone) in this section, and generally in NW European sections. Importantly, it falsifies the description of a negative $\delta^{13}C$ excursion spanning the Pl/To boundary, and by extension our understanding of the Pl/To event.

6.2. Condensation/hiatus in lowermost Toarcian

The negative $\delta^{13}C_{org}$ excursion observed in the lower *tenuicostatum* zone (lowermost Toarcian) in the reference record of the Mochras core (Xu et al., 2018; Storm et al., 2020; Fig. 7), in Morocco (Bodin et al., 2016), Chile (Fantasia et al., 2018), Portugal (Hesselbo et al., 2007; Fantasia et al., 2019), and Argentina (Al-Suwaidi et al., 2022) suggests nevertheless that a global perturbation of the carbon cycle occurred during this time interval. However, differences in the shape, amplitude, and relative thickness varies significantly among these sections. We here advocate that this difference is linked to the frequent presence of condensation or hiatus in the lowermost Toarcian induced by the outstanding environmental and sediment supply changes accompanying the unfolding of the Pl/To event.

In the Dades Valley (Central High Atlas, Morocco), outstanding exposure allows to visualize the effect of these drastic changes during the Pl/To transition and replace them within a detailed context of sea-level change (Krencker et al., 2020, 2022; Andrieu et al., 2022; Fig. 11). The Pl/To boundary slightly postdates the onset of environmental perturbations, as recorded by decreasing neritic carbonate production and export to the basin, leading to the formation of the "transition beds" (originally defined as the "couches de passage" in Portugal by Mouterde, 1955; cf. da Rocha et al., 2016; Bodin et al., 2016). This is coeval to the onset of nutrient level rise in the seawater (Bodin et al., 2010) and increased continental weathering (Krencker et al., 2020; step #1–2 in Fig. 11). During the earliest Toarcian, escalation of environmental deterioration led to the shrinking of neritic carbonate production that lost its capacity to shed carbonate mud into the basin (step #3–4 in Fig. 11). This resulted in the formation of a cryptic condensation surface in deep-water setting (Krencker et al., 2022; Andrieu et al., 2022). Ultimately, the carbonate factory collapsed (step #5 in Fig. 11) and was replaced by voluminous siliciclastic supply fed by a deltaic system (step #5–6 in Fig. 11). This last step occurred concomitantly to a significant (ca. 40 m) sea-level fall as deduced from karstification on top of the Choucht carbonate platform and geometric relationship with the following siliciclastic deposits, showing continental deposits 40 m below the top of this platform (Krencker et al., 2020, 2022). This accounts for further condensation in the lowermost Toarcian in localities that were far away from the deltaic system, i.e., from the sediment supply source.

With the exception of the vigorous coarse siliciclastic sedimentation in the aftermath of the carbonate collapse, a similar scenario can also be suggested in the Lusitanian Basin (Pittet et al., 2014), as well as inferred for numerous circum-Tethys localities where offshore sedimentation during the Pl/To transition is characterized by first a decrease of carbonate content (equivalent of the "transition beds"), followed by an abrupt loss of carbonate content (e.g. Brunel et al., 1999; Mattioli and Pittet, 2004; Danise et al., 2019). In the Peniche section, condensation at the top of the last carbonate "transition" bed (bed 15e) is well known (Mouterde, 1955; Pittet et al., 2014; da Rocha et al., 2016) and marked by an unusual concentration of belemnite rostra (Rita et al., 2019). It is also clearly visible from the abrupt shift of clay mineral assemblage and trace elements concentration at the top of the bed, as well as a ca. 3‰ abrupt negative shift of $\delta^{13}C_{org}$ values (Fantasia et al., 2019). A significant amount of time must therefore be lacking at the top surface of bed 15e, changing the perspective about the paleoenvironmental information derived from this section for the Pl/To event. It is however impossible to quantify directly the amount of time that is missing or condensed here. Nevertheless, by analogy to the learnings from the Central High Atlas Basin (Krencker et al., 2022), one can suspect that the absence of coarse siliciclastic sediment supply during the earliest Toarcian in the Peniche area would imply that the top of Bed 15e is even more condensed that its equivalent in the Dades Valley. Given the collapse of neritic carbonate production during the Pl/To event, only sections close to an entry point of siliciclastic sediments show an almost complete record of the Pl/To event, whereas condensation time increases with relative distance to this entry point due to the time involved in the progradation of the siliciclastic system (Krencker et al., 2022). In the Cleveland basin, a small negative $\delta^{13}C_{org}$ excursion is observed in the lowermost Toarcian, ca. 1 m above the Pl/To boundary (Littler et al., 2010), within an overall transgressive context (Hesselbo and Jenkyns, 1998). This excursion is strongly correlated to enrichment of organic matter content in the sediments, suggesting that it might reflect admixing of marine organic matter in the TOC rather than a genuine perturbation of the global carbon cycle (e.g. Suan et al., 2015). We therefore postulate that this negative excursion is not to be correlated to the lowermost Toarcian negative $\delta^{13}C$ excursion as observed in Morocco and in the Mochras core. Rather, we here suggest that the base of the Polymorphum chronozone is absent if the Hawsker Bottoms section, and that only the uppermost part of the Pl/To negative $\delta^{13}C$ excursion, i.e. the positive trend toward pre-excursion values, is recorded. This is consistent with the positive trend of $\delta^{13}C$ values measured from

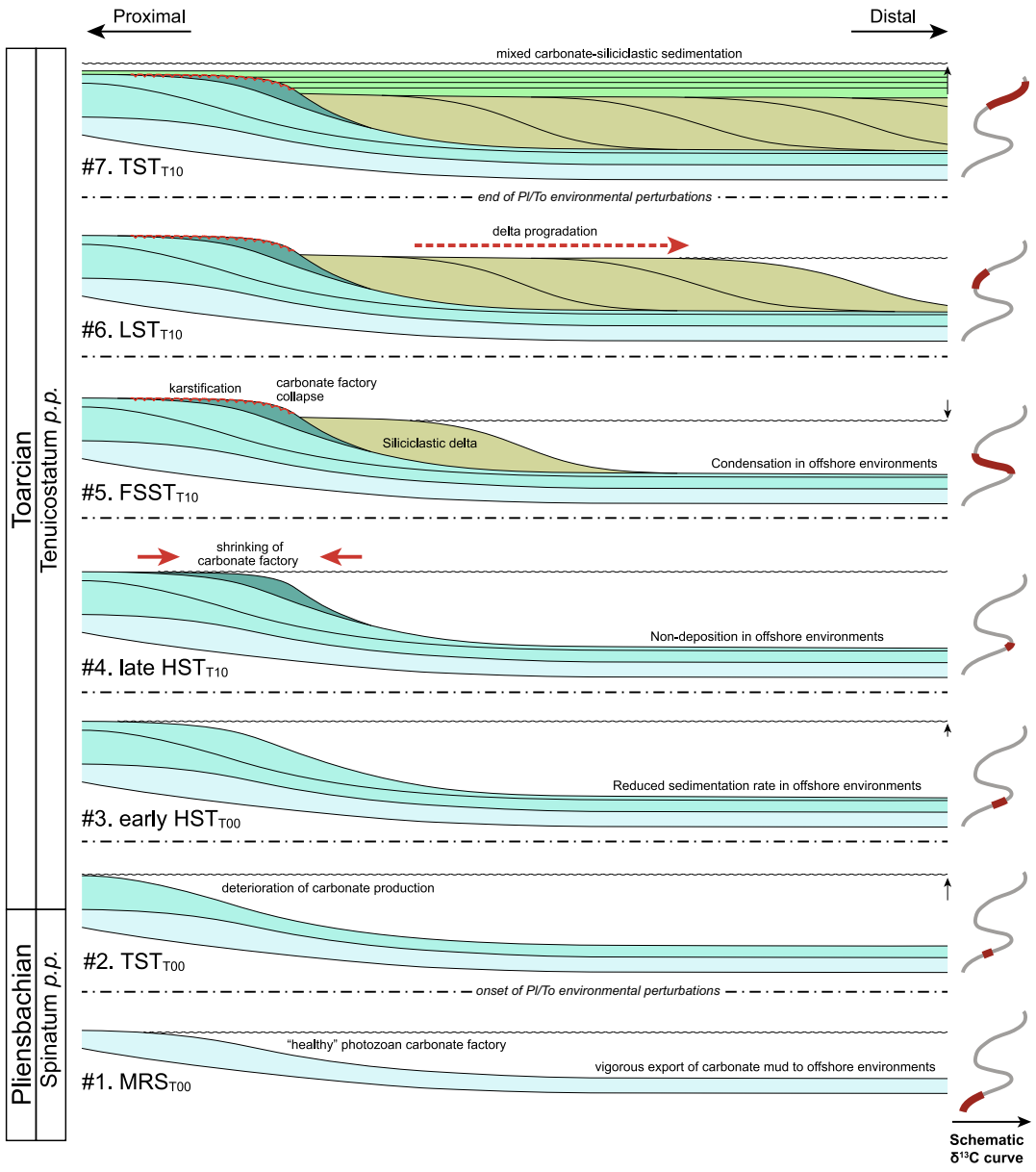

Fig. 11. Schematic model of the evolution of sedimentation regime and stacking pattern across the Pliensbachian/Toarcian boundary in the Dades Valley, Morocco (after observations and interpretations in Krencker et al., 2022, and Andrieu et al., 2022). On the right hand-side, the time interval represented by each step relative to the schematic $\delta^{13}C_{org}$ curve of the Pliensbachian – Toarcian transition (cf. Fig. 13) is marked with a thick red line. Step #1 represents the "unperturbed" situation during the latest Pliensbachian, with a vigorous Photozoan carbonate factory. The environmental perturbation at the origin of the Pl/To event lead to a progressive decrease of neritic carbonate production accompanied by a shoreline retrogradation during relative sea-level rise (Step #2). A progressive reduction of neritic carbonate export into basin, together with increased siliciclastic mud flux and decreased relative sea-level rise, lead to renewed progradation but reduced sedimentation rates in the basin (Step #3). This step corresponds to the formation of the "transition beds". In the final stage of altered neritic carbonate production (Step #4), the carbonate production area shrinks drastically, leading to a halt of carbonate export in the basin. This initiates the creation of a hiatal surface at the top of the "transition beds". The "coup-de-grâce" to the neritic carbonate production is provided by a 40 m sea-level fall accompanied by the arrival of coarse siliciclastic sediments at the shoreline (Step #5). Away from the entry point of siliciclastic sediments, little to no sedimentation occurs as it takes time to the siliciclastic sediments to be transported into distal marine settings (Step #6). At the end of the Pl/To event, carbonate production resumes in a mixed carbonate-siliciclastic mode (Step #7). This occurs during a strong relative sea-level rise, inducing a flooding of the entire region. (For interpretation of the references to color in this figure legend, the reader is referred to the web version of this article.)

belemnite rostra in this part of the section (Korte et al., 2015). This also agrees with observations from Morocco that indicate a relative sea-level rise during the end of the Pl/To event and its immediate afterwards.

The effect of differential sediment supply in the earliest Toarcian can be well-pictured from the comparison of the $\delta^{13}C_{org}$ record from the Bou Oumardoul n'Imazighn section (Dades Valley, Morocco), the Mochras core, and the Peniche section (Fig. 12). The sections from the Dades valley show an overall higher sediment accumulation rate compared to these two other European sections, which are generally considered as expanded Toarcian records in the available literature (Ruhl et al., 2016). In Fig. 12, in order to represent a similar relative thickness for the T-OAE, a 2× and 5× vertical exaggeration has to be applied to the Mochras core and Peniche section, respectively. Yet, even with this vertical exaggeration, the relative thickness of the *polymorphum* zone in the Bou Oumardoul n'Imazighn section is twice as much than in the two other records. This is even more remarkable given that within the

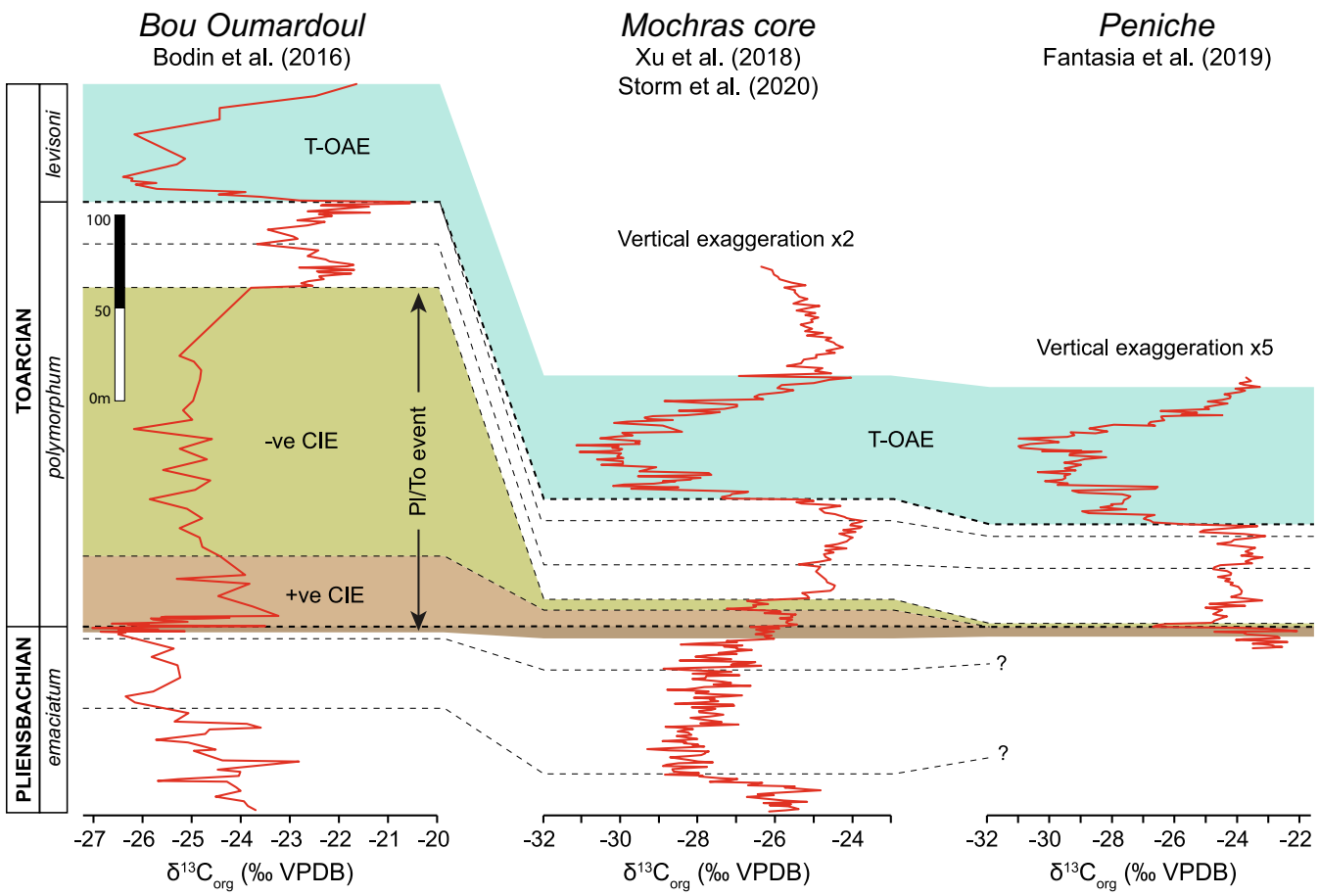

Fig. 12. Correlation of uppermost Pliensbachian – early Toarcian bulk organic matter $\delta^{13}C$ curve between the Bou Oumardoul n'Imazighn section (Morocco), the Mochras core (Wales), and the Peniche section (Portugal). Data are from Bodin et al. (2016), Xu et al. (2018), Fantasia et al. (2019), and Storm et al. (2020). In order to obtain a similar relative thickness of the T-OAE interval in the three records, a 2× and 5× vertical exaggeration was applied to the Mochras core and Peniche section, respectively. The position of the Pliensbachian/Toarcian boundary in the Mochras core is the same as in Fig. 7. This correlation highlights the highly expanded character of the *polymorphum* zone in the Bou Oumardoul n'Imazighn section. When not affected by hiatus such as in the Peniche section, the Pl/To event is characterized by an initial positive carbon isotope excursion spanning the Pliensbachian/Toarcian boundary, followed by a negative carbon isotope excursion in the lowermost Toarcian. "+ve CIE": Positive carbon isotope excursion; "-ve CIE": Negative carbon isotope excursion.

polymorphum zone, the top of the Tagoudite Formation coincides with a significant bypass level due to strong progradational pattern associated with a maximum regressive surface (MRS_{T10} in Krencker et al., 2022), and that the top of the Polymorphum chronozone is absent in this section due to a 50 m relative sea-level fall and the creation of an incised valley prior to the onset of the T-OAE (Krencker et al., 2019). The highly expanded character of the Bou Oumardoul n'Imazighn section is a direct consequence of its peculiar paleo-location: at the toe-of-slope of the Pliensbachian Choucht carbonate platform (Andrieu et al., 2022) and at the delta front of the earliest Toarcian siliciclastic system (Krencker et al., 2022). Thus, despite a 40 m sea-level fall and the carbonate factory collapse during the earliest Polymorphum chronozone (Krencker et al., 2022), this peculiar setting implies high available accommodation space and elevated sediment supply during the earliest Toarcian. To our knowledge, the Bou Oumardoul n'Imazighn section therefore provides the most complete and expanded record of the earliest Toarcian environmental perturbation.

Acknowledging condensation/hiatus level and highly fluctuating sedimentation rates within and among each section, the chemostratigraphic correlation presented in Fig. 12 clearly highlights the similarities of the three $\delta^{13}C_{org}$ record trends in the *polymorphum* zone, nicely exemplified by the two small $\delta^{13}C$ positive excursions in the upper *polymorphum* zone that terminate a long-term positive trend initiated in the upper *spinatum* zone. In the Bou Oumardoul n'Imazighn section, the upper part of the second small $\delta^{13}C_{org}$ positive excursion is however absent due to the hiatus associated with the 50 m sea-level fall during the latest Polymorphum chronozone (SB_{T20} in Krencker et al., 2022).

In the lower part of the *polymorphum* zone, a negative $\delta^{13}C_{org}$ excursion is observed and associated with the Pl/To event. The exact timing of this negative excursion differs nevertheless between the three records (Fig. 12). This can be explained by a misplacement of the Pl/To boundary in the Mochras core and the hiatus/condensation on top of bed 15e in the Peniche section. Hence, in the Mochras core, the position of this boundary has so far been based on the first occurrence of *Dactylioceras* ammonites at 863.50 m downcore (Ivimey-Cook, 1971). This attribution is nevertheless speculative given that the last occurrence of amaltheid ammonites is reported at 868.17 m (Ivimey-Cook, 1971). This is due to a 4.67 m ammonite-barren interval within this part of the core, implying an uncertainty range for the position of the Pliensbachian/Toarcian boundary using only ammonite biostratigraphy. In a recent high-resolution nannofossil study, Menini et al. (2021) have placed the base of the NJT5c nannofossil subzone (first occurrence of the nannofossil *Zeugrhabdothus erectus*) in the Mochras core at 868.32 m. This is 15 cm below the last occurrence of Amaltheids in this core. Given that the base of the NJT5c subzone is situated slightly above (ca. 0.5 m) the Pliensbachian/Toarcian boundary in Peniche section (da Rocha et al., 2016; Ferreira et al., 2019), which is the GSSP for the Toarcian stage, the last appearance of Amaltheid ammonites and first appearance of *Z. erectus* seems to be almost contemporaneous over the Euro-Boreal realm. Therefore, we adopt here the last appearance of Amaltheid

ammonites as a better indicator for the Pl/To boundary in the Mochras core. By doing this, a consistent $\delta^{13}C_{org}$ picture emerges between the Mochras core and the Bou Oumardoul n'Imazighn section. The Pl/To boundary is thus characterized by a positive trend in $\delta^{13}C_{org}$ values peaking in the lowermost *polymorphum* zone, followed by a negative $\delta^{13}C_{org}$ excursion associated with the upper part of the Pl/To event record. This correlation also highlights that in the Peniche section, this peak of $\delta^{13}C_{org}$ values (and also likely the lower part of the Pl/To negative excursion) is however absent due to the hiatus/condensation associated with the top of Bed 15e.

6.3. Was the Pliensbachian/Toarcian boundary event triggered and ended by volcanism?

The origin of the Pl/To event is often attributed to a first eruptive phase of the Karoo-Ferrar large igneous province (LIP), as evidenced by a Hg anomaly occurring at this stratigraphic interval in numerous localities (Percival et al., 2015; Al-Suwaidi et al., 2022; Ruhl et al., 2022). Nevertheless, in the reference section of Peniche, a high-resolution Hg investigation failed at reproducing a significant Hg/TOC anomaly across the Pl/To event (Fantasia et al., 2019). Although the Hg concentration data from the Bou Oumardoul n'Imazighn section shows an enrichment across the Pl/To boundary (Fig. 8), once normalized with TOC values, no anomalous Hg enrichment can be observed except for one point in the uppermost Ouchbis Formation. The Hg/TOC values are slightly higher in the Tagoudite Formation compared to the Ouchbis Formation, but this seems to be linked to the relatively low TOC values in this Formation ($< 0.2\%$) rather than to a genuine enrichment of Hg in the environment. Contrary to the T-OAE, the presence of Hg anomaly across the Pl/To boundary is therefore not ubiquitous. The absence of such Hg anomaly is however not on its own disproving a volcanic trigger for the Pl/To event, as not all types of volcanism are expected to create global enrichment of Hg in the environment (Percival et al., 2021). Moreover, the presence of a hiatus at the top of the Bed 15e could also explain the rather subdued Hg anomaly across the Pl/To interval in the Peniche section.

Another factor of uncertainty arises from the study of Them et al. (2019) who questioned the validity of Hg enrichment in sedimentary rocks as a tracer for global volcanism. Hence, these authors argued that Hg anomalies are primarily caused by change in the flux of terrestrially sourced materials. The Bou Oumardoul n'Imazighn dataset challenges however this claim. As a matter of fact, the Hg concentration anomaly across the Pl/To boundary is recorded in offshore limestone-marl alternations (carbonate content between 40% and 80%; Krencker et al., 2022), whereas the following siliciclastic-dominated sediments (carbonate content around 20%; Krencker et al., 2022) from the lower Tagoudite Formation shows no peculiar Hg enrichment, as would be expected if Hg concentration would be primarily correlated to terrestrial clastic flux. On the contrary, it could be argued that the absence of any significant Hg anomaly in the lowermost Toarcian of Morocco could be induced by the very high sedimentation rates observed in the deltaic deposits of the lower Tagoudite Formation. In a Hg supply-limited environment, such high terrestrial sedimentation rates would thus dampen the Hg signal rather than being at the origin of anomalous enrichment.

The absence in some sections of significant Hg anomalies across the Pl/To event can thus be explained by local factors. Therefore, given the well-established link between large igneous province eruptions and mass extinction events (e.g., Bond et al., 2014), and the available Hg data, unusual volcanic activity across the Pl/To boundary is the best working hypothesis to explain the environmental disaster at the dawn of the Toarcian age.

The end of the Pl/To event coincides with the first small $\delta^{13}C_{org}$ positive excursion, as well as with scattered Hg/TOC anomalies in the lowermost Tafraout Formation (Fig. 8). According to the recent dating of the onset of the T-OAE (*tenuicostatum/serpentinum* zonal boundary) at $182.77 + 0.11/- 0.15$ Ma (Al-Suwaidi et al., 2022), it appears that numerous dating derived from Karoo igneous rocks pre-dates the onset of the T-OAE by ca. 400 kyr and, interestingly, correlate to the same first small $\delta^{13}C_{org}$ positive excursion in the Mochras core (cf. Fig. 5 in Al-Suwaidi et al., 2022, and references therein), as well as with a small Hg/TOC enrichment in the Mochras core (Percival et al., 2016; Xu et al., 2018: Ruhl et al., 2022). A second eruptive phase of the Karoo-Ferrar LIP during the Polymorphum chronozone seems thus to be coeval with the end of the Pl/To event. Sequence stratigraphy analyses from the Moroccan record shows that this $\delta^{13}C_{org}$ positive excursion coincides with the onset of a significant transgression in this basin (TST_{T10}; Krencker et al., 2022; Fig. 8). The coexistence between the two events potentially suggests that this transgression and the end of the Pl/To event are related to a global sea-level rise induced by volcanic-driven environmental change.

6.4. An updated scenario for the Pliensbachian/Toarcian boundary event

Taking into account the outcome of the previous discussion, we propose a new scenario for the Pl/To event based on a combined sedimentological and geochemical approach, and highlight numerous unknowns that derive from the understanding of a highly incomplete sedimentary record across the Pl/To boundary in many localities (Fig. 13).

The onset of carbonate production decline in both pelagic and neritic carbonate factories (as deduced from nannofossil analysis and the occurrence of the "transition beds" in numerous Tethyan localities, respectively) indicates that the onset of the Pl/To event slightly precedes the Pl/To boundary (Suan et al., 2008; Bodin et al., 2016; Menini et al., 2021; Peti et al., 2021). In Morocco, the base of the Toarcian stage coincides with the MFS_{T00} (Krencker et al., 2022). The initial part of the Pl/To event is therefore associated with a transgression occurring in the latest Pliensbachian. This transgression is accompanied by a positive excursion of $\delta^{13}C_{org}$ value. Such positive carbon isotope shift is usually interpreted to reflect enhanced organic matter burial on a global scale (Scholle and Arthur, 1980), in agreement with sulfur isotope record from Japan which implies increased marine organic matter and pyrite burial during the Pl/To event (Chen et al., 2022). No peculiar enrichment in TOC is however observed in the European reference sections of Peniche (Fantasia et al., 2019), in the Mochras core (Storm et al., 2020), or in Morocco (e.g., Bodin et al., 2010; Ait-Itto et al., 2017; see also Fig. 8). TOC enrichment related to the Pl/To event is nevertheless reported from Japan (Kemp et al., 2022), Argentina (Al-Suwaidi et al., 2022), and could also be inferred from northwest America data (Them et al., 2017a). This suggests that the Panthalassa Ocean could have acted as the principal carbon sink during the Pl/To event due to the development of bottom-water anoxia (Kemp et al., 2022). This can be directly linked to increased global weathering rates and oceanic nutrient level during the Pl/To event (Bodin et al., 2010; Brazier et al., 2015; Percival et al., 2016; Them et al., 2017b; Krencker et al., 2020).

As discussed earlier, the Pl/To event is potentially driven by unusual volcanic activity, probably related to a first pulse of the Karoo-Ferrar LIP. Global sea-level rise and increased burial of organic matter is commonly observed during other episodes of environmental upheaval linked to LIP activity (e.g., Keller et al., 2004; Jenkyns, 2010). Depending on the balance and timing between greenhouse gases emission from volcanic activity and global carbon burial, cooling episodes during OAEs can occur if the latter outpaces the former (Jenkyns, 2018). The OAE 2 is one of the best documented examples of such a scenario with the occurrence of the Plenus cold event coinciding with a first peak of the $\delta^{13}C$ record (Jarvis et al., 2011) and a pronounced sea-level fall at its base (e.g., Janetschke and Wilmsen, 2014), potentially indicating the transient development of polar ice during this event. Interestingly, the second part of the Pl/To event corresponds as well to a large (ca. 40 m) sea-level fall initiated at the climax of a positive $\delta^{13}C$ excursion (Krencker et al., 2022). A parallel could thus be drawn between these two events, suggesting cooling-driven sea-level fall during the second

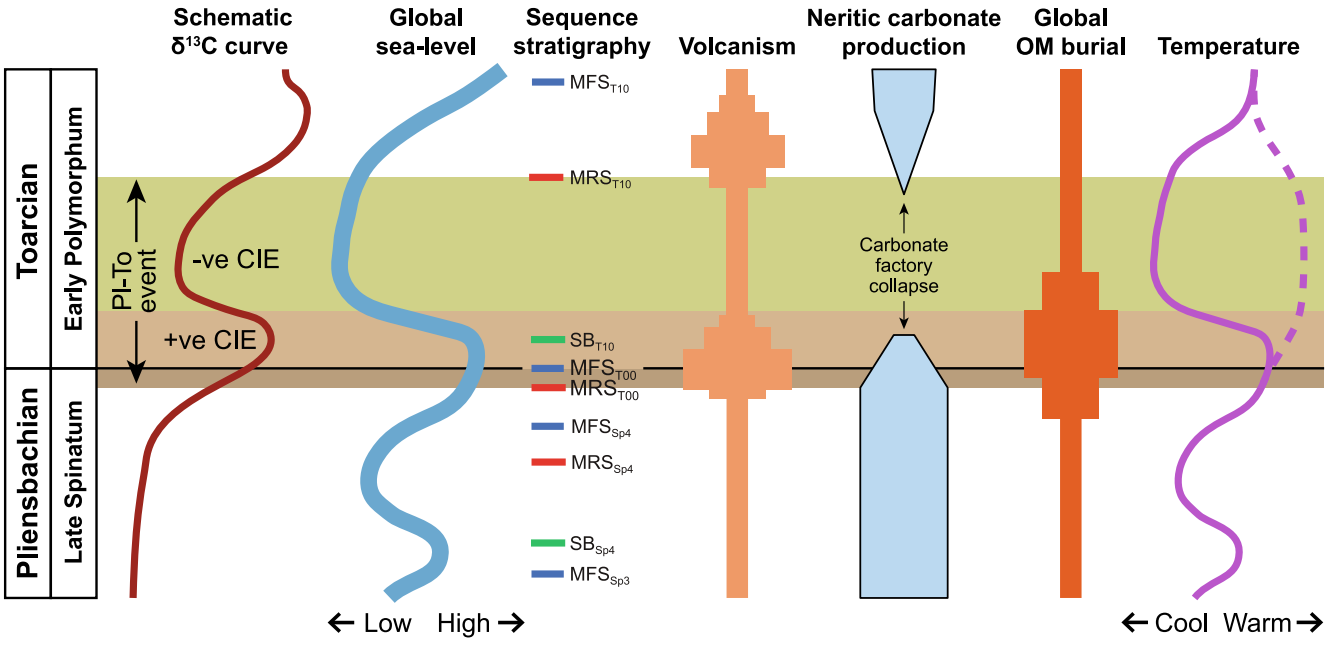

Fig. 13. Summary of paleoenvironmental changes taking place during the Pliensbachian – Toarcian transition. No exact time-scale is implied on the vertical axis. The color shading of the Pl/To event C-isotope interval is the same as in Fig. 12. For the temperature evolution curve, two options are presented: cooling or warming during the Pl/To event negative $\delta^{13}C$ excursion. The cooling scenario is the most likely as it coincides with a 40 m sea-level fall interval (see text for discussion). Abbreviations: "+ve CIE": Positive carbon isotope excursion; "-ve CIE": Negative carbon isotope excursion.

part of the Pl/To-event, which is characterized by a negative $\delta^{13}C$ excursion that could be linked to a diminution of global organic carbon burial.

There is however no clear evidence for an earliest Toarcian cooling in the literature. On the contrary, available data suggest that warming might have accompanied the unfolding of the Pl/To event. Hence, in the Peniche section, in the condensed top of bed 15e that encapsulates most of the time equivalent of this sea-level fall episode, a $\delta^{18}O$ negative excursion in brachiopod shells was interpreted by Suan et al. (2008) as a major rise of seawater temperature during this event. According to these authors, this interpretation is supported by ammonite migration pattern indicating a northward expansion of Tethyan fauna. Additionally, $\delta^{18}O$ values measured in belemnite rostra in the Almonacid de la Cuba section (Spain; Comas-Rengifo et al., 2010), and TEX_{86} data from La Cerradura section (Spain; Ruebsam et al., 2020) also suggest seawater warming during the Pl/To event. This is in opposition to $\delta^{18}O$ values measured in brachiopod shells from the Barranco de la Cañada (Spain) and Fonte Coberta/Rabacal (Portugal) sections that suggest relatively cool temperature during the earliest Toarcian (Ullmann et al., 2020). Nevertheless, for the brachiopod and belemnite $\delta^{18}O$ values, it is also questionable whether those only reflect paleotemperature change. Hence, they could alternatively also be interpreted as reflecting a lowering of the seawater $\delta^{18}O$ value due to the enormous increase of riverine runoff during the unfolding of the Pl-To event in this region (Krencker et al., 2020; Fantasia et al., 2019), although the presence of stenohaline organisms such as brachiopods excludes any important drop of seawater salinity (Ullmann et al., 2020). The chronostratigraphic attribution in La Cerradura section is also questionable due to a scarcity in biostratigraphic markers as well as the very reduced thickness of the *polymorphum* zone in this section. In the light of the learning of the present study, the absence of a negative $\delta^{13}C$ excursion in the lowermost Toarcian of La Cerradura section suggests that the hiatus at the top of the last limestone bed (2–4 m above the Pl/To boundary; Ruebsam et al., 2020) corresponds to the top of the "transition beds", implying that the upper part of the Pl/To event, as well as most of the *polymorphum* zone, is missing in this section. In this case, it is nevertheless important to note that a positive excursion of TEX_{86} values spans the Pl/To boundary in this section; this latter indicates a warming event that can be linked to increased greenhouse conditions due to volcanic activity in the first part of the Pl/To event. Given that the Pl/To negative carbon isotope excursion is associated with a 40 m sea-level fall, a cooling event is also more likely to have taken place during this time interval rather than a warming event, in agreement with the high-resolution brachiopod $\delta^{18}O$ values presented by Ullmann et al. (2020). As a matter of fact, such an ample and rapid sea-level fluctuation can only be confidently explained by glacio-eustatism; a mechanism already thought to have operated in the late Pliensbachian and the early Toarcian (Korte and Hesselbo, 2011; Krencker et al., 2019; Ruebsam et al., 2019). In the opposite case, aquifer-eustasy should be invoked, but a recent study has casted serious doubt about the capacity of this mechanism to induce eustatic sea-level fluctuation higher than 5 m of amplitude (Davies et al., 2020).

The end of the Pl/To event is associated with a maximum regressive surface (MRS_{T10} in Krencker et al., 2022) and the onset of a first minor positive $\delta^{13}C_{org}$ excursion observed as well in the European records (Fig. 12). Renewed climate warming and sea-level rise can thus be postulated to have taken place at the termination of this event. As discussed earlier, an eruptive phase of the Karoo-Ferrar LIP seems to be at the origin of this environmental overturn.

7. Conclusions

The Pliensbachian/Toarcian transition was a time interval marked by pronounced environmental changes. During the latest Pliensbachian, a pronounced progradation pattern is observed in numerous basins due to a long-term global sea-level lowstand combined with high-frequency sea-level fluctuations likely paced by glacio-eustasy. As a result, only localities situated in distal basin settings are likely to present a complete record of the Spinatum chronozone. During the earliest Toarcian, a global collapse of neritic carbonate production occurred in combination with a rapid eustatic sea-level fall. Combined with this, the absence of sufficient siliciclastic sediment supply also favoured sediment starvation in offshore settings whereas erosion/karstification took place in proximal settings. This combination of causes explains the ubiquitous presence of hiatuses and condensation horizons in the sedimentary record,

impairing an accurate and complete record of the Pl/To event in numerous localities.

A comparison of the $\delta^{13}C_{org}$ records of the Mochras core (Wales) and the Bou Oumardoul n'Imazighn section (Morocco), which are the two most expanded records of the Pliensbachian/Toarcian transition, shows that the Pl/To event is characterized by a twofold $\delta^{13}C_{org}$ evolution. Its lower part is thus characterized by a small positive $\delta^{13}C_{org}$ excursion spanning the Pl/To boundary. This occurs during a time of pronounced sea-level rise. The upper part of the Pl/To event is characterized by a negative $\delta^{13}C_{org}$ excursion in the lowermost Toarcian that is concomitant to a large sea-level fall and halt in carbonate sedimentation. This combination of causes explains that this time interval is often not preserved. The end of the Pl/To event is characterized by renewed sedimentation in most basin and relative sea-level rise.

Due to the widespread hiatus/condensation occurring at the Pliensbachian/Toarcian transition, there is currently no high-resolution paleotemperature reconstruction available for this entire time interval. A warming pulse can nevertheless be inferred for the first part of the Pl/To event, whereas the large sea-level fall occurring in its second part argues for a succeeding cooling event, likely caused by enhanced burial of organic matter in the Panthalassa regions. Both onset and termination of the Pl/To event seems to be related to volcanic activity, although further investigations are needed to confirm this hypothesis, especially for the termination of the event.

In general, this study highlights the difficulty of getting complete sedimentary records from chronostratigraphic interval that have experienced significant sediment supply and sea-level variations, peculiarly before the late Mesozoic, when a vigorous pelagic carbonate factory was not yet established. The uncertainties generated by these unsteady conditions can however be lifted by a basin scale approach combining sequence stratigraphy and high-resolution chronostratigraphy.

Declaration of Competing Interest

The authors declare that they have no known competing financial interests or personal relationships that could have appeared to influence the work reported in this paper.

Data availability

Data will be made available on request.

Acknowledgments

We warmly thank Myette Guiomar and Didier Bert from the Reserve Géologique de Haute-Provence for providing fieldwork and sampling permits, as well as their continuous scientific support. We also thank Stephen Hesselbo and an anonymous reviewer for their comments and suggestions that have helped to improve this manuscript. This research was financed by the Independent Research Fund Denmark (DFF, grant n° 9040-00188B) to SB.

Appendix A. Supplementary data

Supplementary data to this article can be found online at https://doi.org/10.1016/j.palaeo.2022.111344.

References

Ait-Itto, F.-Z., Price, G.D., Ait Addi, A., Chafiki, D., Mannani, I., 2017. Bulk-carbonate and belemnite carbon-isotope records across the Pliensbachian-Toarcian boundary on the northern margin of Gondwana (Issouka, Middle Atlas, Morocco). Palaeogeogr. Palaeoclimatol. Palaeoecol. 466, 128–136.

Al-Suwaidi, A.H., Ruhl, M., Jenkyns, H.C., Damborenea, S.E., Manceñido, M.O., Condon, D.J., Angelozzi, G.N., Kamo, S.L., Storm, M., Riccardi, A.C., Hesselbo, S.P., 2022. New age constraints on the lower Jurassic Pliensbachian-Toarcian Boundary at Chacay Melehue (Neuquén Basin, Argentina). Sci. Rep. 12 (1), 4975.

Andrieu, S., Krencker, F.-N., Bodin, S., 2022. Anatomy of a platform margin during a carbonate factory collapse: implications for the sedimentary record and sequence stratigraphy interpretation of poisoning events. J. Geol. Soc. 179, jgs2022-005.

Arnaud, H., 2005. The South-East France Basin (SFB) and its Mesozoic evolution. In: Adatte, T., Arnaud-Vanneau, A., Arnaud, H., Blanc-Aletru, M.C., Bodin, S., Carrio-Schaffhauser, E., Föllmi, K.B., Godet, A., Raddadi, M.C., Vermeulen, J. (Eds.), The Hauterivian - Lower Aptian Sequence Stratigraphy from Jura Platform to Vocontian Basin: A Multidisciplinary Approach, pp. 5–28.

Baghli, H., Mattioli, E., Spangenberg, J.E., Bensalah, M., Arnaud-Godet, F., Pittet, B., Suan, G., 2020. Early Jurassic climatic trends in the south-Tethyan margin. Gondwana Res. 77, 67–81.

Bassoulet, J.-P., Elmi, S., Poisson, F., Cecca, F., Belion, Y., Guiraud, R., Baudin, F., 1993. Mid Toarcian. In: Dercourt, J., Ricou, L.E., Vrielynck, B. (Eds.), Atlas Tethys, Palaeoenvironmental Maps. Becip-Franlab, Rueil-Malmaison, France, pp. 63–80.

Blomeier, D.P.G., Reijmer, J.J.G., 1999. Drowning of a Lower Jurassic Carbonate Platform: Jbel Bou Dahar, High Atlas, Morocco. Facies 41, 81–110.

Bodin, S., Godet, A., Vermeulen, J., Linder, P., Föllmi, K.B., 2006. Biostratigraphy, sedimentology and sequence stratigraphy of the latest Hauterivian - early Barremian drowning episode of the Northern Tethyan margin (Altmann Member, Helvetic nappes, Switzerland). Eclogae Geol. Helv. 99 (2), 157–174.

Bodin, S., Hönig, M.R., Krencker, F.-N., Danisch, J., Kabiri, L., 2017. Neritic carbonate crisis during the early Bajocian: divergent responses to a global environmental perturbation. Palaeogeogr. Palaeoclimatol. Palaeoecol. 468, 184–199.

Bodin, S., Krencker, F.-N., Kothe, T., Hoffmann, R., Mattioli, E., Heimhofer, U., Kabiri, L., 2016. Perturbation of the carbon cycle during the late Pliensbachian – early Toarcian: new insight from high-resolution carbon isotope records in Morocco. J. Afr. Earth Sci. 116, 89–104.

Bodin, S., Mattioli, E., Fröhlich, S., Marshall, J.D., Boutib, L., Lahsini, S., Redfern, J., 2010. Toarcian carbon isotope shifts and nutrient changes from the Northern margin of Gondwana (High Atlas, Morocco, Jurassic): palaeoenvironmental implications. Palaeogeogr. Palaeoclimatol. Palaeoecol. 297 (2), 377–390.

Bond, D.P.G., Wignall, P.B., Keller, G., Kerr, A.C., 2014. Large igneous provinces and mass extinctions: an update. In: Keller, G., Kerr, A.C. (Eds.), Volcanism, Impacts, and Mass Extinctions: Causes and Effects. Geological Society of America, pp. 29–55.

Brame, H.-M.R., Martindale, R.C., Ettinger, N.P., Debeljak, I., Vasseur, R., Lathuilière, B., Kabiri, L., Bodin, S., 2019. Stratigraphic distribution and paleoecological significance of early Jurassic (Pliensbachian-Toarcian) lithiotid-coral reefal deposits from the Central High Atlas of Morocco. Palaeogeogr. Palaeoclimatol. Palaeoecol. 514, 813–837.

Brazier, J.-M., Suan, G., Tacail, T., Simon, L., Martin, J.E., Mattioli, E., Balter, V., 2015. Calcium isotope evidence for dramatic increase of continental weathering during the Toarcian oceanic anoxic event (Early Jurassic). Earth Planet. Sci. Lett. 411, 164–176.

Brunel, F., Rey, J., Cubaynes, R., Deconinck, J.-F., Emmanuel, L., Lachkar, G., 1999. Sedimentology, mineralogy, geochemistry and palynology of Domerian systems tracts of the northern Quercy (NE Aquitain Basin). Bull. Soc. Géol. France 170 (4), 475–486.

Caloo, B., 1970. Biostratigraphie de l'Aalenien et de la base du Bajocien dans la région de Digne (Basses-Alpes, France). Comptes Rendus de l'Académie des Sciences de Paris 271, 1938–1940.

Carbone, F., 1984. Evoluzione tettonico-sedimentaria delle unità carbonatiche centro-appenniniche durante il Meso- Cenozoico. Centro di Studio per la Geologia dell'Italia Centrale. Centro di Studio per la Geologia dell'Italia Centrale. CNR, Roma.

Caruthers, A.H., Smith, P.L., Gröcke, D.R., 2013. The Pliensbachian-Toarcian (Early Jurassic) extinction, a global multi-phased event. Palaeogeogr. Palaeoclimatol. Palaeoecol. 386, 104–118.

Catuneanu, O., Galloway, W.E., Kendall, C.G.S.C., Miall, A.D., Posamentier, H.W., Strasser, A., Tucker, M.E., 2011. Sequence stratigraphy: methodology and nomenclature. Newsl. Stratigr. 44 (3), 173–245.

Cecca, F., Macchioni, F., 2004. The two early Toarcian (Early Jurassic) extinction events in ammonoids. Lethaia 37, 35–56.

Célini, N., Callot, J.-P., Ringenbach, J.-C., Graham, R., 2020. Jurassic salt tectonics in the SW sub-alpine fold-and-thrust belt. Tectonics 39 (10) e2020TC006107.

Chen, W., Kemp, D.B., Newton, R.J., He, T., Huang, C., Cho, T., Izumi, K., 2022. Major sulfur cycle perturbations in the Panthalassic Ocean across the Pliensbachian-Toarcian boundary and the Toarcian Oceanic Anoxic Event. Glob. Planet. Chang. 215, 103884.

Clifton, H.E., 2006. A Reexamination of Facies Models for Clastic Shorelines. In: Posamentier, H.W., Walker, R.G. (Eds.), Facies Models Revisited. SEPM Society for Sedimentary Geology, pp. 293–337.

Coadou, A., Beaudoin, B., Mouterde, R., 1971. Variations lithologiques et correlations stratigraphiques dans le Lias moyen et superieur de Barles et du Plateau de Chine (Alpes de Haute-Provence). Bull. Soc. Géol. France, Ser. 7 (Vol. XIII(1-2)), 5–12.

Comas-Rengifo, M.J., Gómez, J.J., Goy, A., Osete, M.L., Palencia-Ortas, A., 2010. The base of the Toarcian (Early Jurassic) in the Almonacid de la Cuba section (Spain). Ammonite biostratigraphy, magnetostratigraphy and isotope stratigraphy. Episodes 33 (1), 15–22.

Csato, I., Catuneanu, O., 2012. Systems tract successions under variable climatic and tectonic regimes: a quantitative approach. Stratigraphy 9 (2), 109–130.

da Rocha, R.B., Mattioli, E., Duarte, L.V., Pittet, B., Elmi, S., Mouterde, R., Cabral, M.-C., Comas-Rengifo, M., Gómez, J., Goy, A., 2016. Base of the Toarcian stage of the lower Jurassic defined by the global boundary stratotype section and point (GSSP) at the Peniche section (Portugal). Episodes 39 (3), 460–481.

Danise, S., Clémence, M.-E., Price, G.D., Murphy, D.P., Gómez, J.J., Twitchett, R.J., 2019. Stratigraphic and environmental control on marine benthic community change through the early Toarcian extinction event (Iberian Range, Spain). Palaeogeogr. Palaeoclimatol. Palaeoecol. 524, 183–200.

Danise, S., Twitchett, R.J., Little, C.T.S., Clémence, M.-E., 2013. The Impact of Global Warming and Anoxia on Marine Benthic Community Dynamics: an example from the Toarcian (Early Jurassic). PLOS ONE 8, e56255.
Davies, A., Gréselle, B., Hunter, S.J., Baines, G., Robson, C., Haywood, A.M., Ray, D.C., Simmons, M.D., van Buchem, F.S.P., 2020. Assessing the impact of aquifer-eustasy on short-term cretaceous sea-level. Cretac. Res. 112, 104445.
De Baets, K., Cecca, F., Guiomar, M., Verniers, J., 2008. Ammonites from the latest Aalenian–earliest Bathonian of La Baume (Castellane area, SE France): palaeontology and biostratigraphy. Swiss J. Geosci. 101, 563–578.
de Graciansky, P.-C., Dardeau, G., Dumont, T., Jacquin, T., Marchand, D., Mouterde, R., Vail, P.R., 1993. Depositional sequence cycles, transgressive-regressive facies cycles, and extensional tectonics; example from the southern subalpine Jurassic basin, France. Bull. Soc. Géol. France 164, 709–718.
de Graciansky, P.C., Durozoy, G., Gigot, P., 1982. Notice Explicative, Carte géologique France (1/50000) Feuille Digne (944). In: BRGM, Orléans, p. 76.
De Lena, L.F., Taylor, D., Guex, J., Bartolini, A., Adatte, T., van Acken, D., Spangenberg, J.E., Samankassou, E., Vennemann, T., Schaltegger, U., 2019. The driving mechanisms of the carbon cycle perturbations in the late Pliensbachian (Early Jurassic). Sci. Rep. 9, 18430.
Dera, G., Brigaud, B., Monna, F., Laffont, R., Pucéat, E., Deconinck, J.-F., Pellenard, P., Joachimski, M., Durlet, C., 2011. Climatic ups and downs in a disturbed Jurassic world. Geology 39 (3), 215–218.
Dera, G., Neige, P., Dommergues, J.-L., Fara, E., Laffont, R., Pellenard, P., 2010. High-resolution dynamics of early Jurassic marine extinctions: the case of Pliensbachian-Toarcian ammonites (Cephalopoda). J. Geol.Soc.Lond. 167, 21–33.
Dromart, G., Allemand, P., Garcia, J.-P., Robin, C., 1996. Variation cyclique de la production carbonatée au Jurassique le long d'un transect Bourgogne-Ardèche, E-France. Bull. Soc.Géol.France 167, 423–433.
Embry, A., Johannessen, E., 1992. T-R sequence stratigraphy, facies analysis and reservoir distribution in the uppermost Triassic-Lower Jurassic succession, western Sverdrup Basin, Arctic Canada. In: Vorren, T.O., Bergsager, E., Dahl-Stamnes, O.A., Holter, E., Johansen, B., Lie, E., Lund, T.B. (Eds.), Arctic Geology and Petroleum Potential. Norwegian Petroleum Society Special Pubication 2, pp. 121–146.
Enay, R., Mangold, C., Cariou, E., Contini, D., Debrand-Passard, S., Donze, P., Gabilly, J., Lefavrais-Raymond, A., Mouterde, R., Thierry, J., 1980. Synthèse paléogéographique du Jurassique francais. Documents du Laboratoire de Géologie de Lyon, Hors Série 5, 1–210.
Ettaki, M., Chellai, E.H., 2005. Le Toarcien inférieur du Haut Atlas de Todrha-Dadès (Maroc): sédimentologie et lithostratigraphie. C. R. Geosci. 337 (9), 814–823.
Ettaki, M., Chellai, E.H., Milhi, A., Sadki, D., Boudchiche, L., 2000. Le passage Lias moyen-Lias superieur dans la region de Todrha-Dades : evenements bio-sedimentaires et geodynamiques (Haut Atlas central, Maroc) - the Middle Lias-Upper Lias crossing in the Todrha-Dades (central High Atlas, Morocco): geodynamic and bio-sedimentary events. Comptes Rendus de l'Academie des Sciences - Series IIA - Earth and Planetary Science 331 (10), 667–674.
Fantasia, A., Adatte, T., Spangenberg, J.E., Font, E., Duarte, L.V., Föllmi, K.B., 2019. Global versus local processes during the Pliensbachian-Toarcian transition at the Peniche GSSP, Portugal: a multi-proxy record. Earth Sci. Rev. 198, 102932.
Fantasia, A., Föllmi, K.B., Adatte, T., Bernárdez, E., Spangenberg, J.E., Mattioli, E., 2018. The Toarcian Oceanic Anoxic Event in southwestern Gondwana: an example from the andean Basin, northern Chile. J. Geol. Soc. 175 (6), 883–902.
Fantasia, A., Mattioli, E., Spangenberg, J.E., Adatte, T., Bernárdez, E., Ferreira, J., Thibault, N., Krencker, F.-N., Bodin, S., 2022. The middle-late Aalenian event: a precursor of the Mesozoic Marine Revolution. Glob. Planet. Chang. 208, 103705.
Ferreira, J., Mattioli, E., Sucherás-Marx, B., Giraud, F., Duarte, L.V., Pittet, B., Suan, G., Hassler, A., Spangenberg, J.E., 2019. Western Tethys Early and Middle Jurassic calcareous nannofossil biostratigraphy. Earth-Science Rev 197, 102908.
Floquet, M., Cecca, F., Mestre, M., Macchioni, F., Guiomar, M., Baudin, F., Durlet, C., Alméras, Y., 2003. Mortalité en masse ou fossilisation exceptionnelle ? Le cas des gisements d'âge toarcien inférieur et moyen de la région de Digne-Les-Bains (Sud-Est de la France). Bull. Soc.Géol. France 174 (2), 159–176.
Franceschi, M., Jin, X., Shi, Z., Chen, B., Preto, N., Roghi, G., Dal Corso, J., Han, L., 2022. High-resolution record of multiple organic carbon-isotope excursions in lacustrine deposits of Upper Sinemurian through Pliensbachian (Early Jurassic) from the Sichuan Basin, China. GSA Bull. https://doi.org/10.1130/B36235.1. In press.
French, K.L., Sepúlveda, J., Trabucho-Alexandre, J., Gröcke, D.R., Summons, R.E., 2014. Organic geochemistry of the early Toarcian oceanic anoxic event in Hawsker Bottoms, Yorkshire, England. Earth Planet. Sci. Lett. 390, 116–127.
Frizon de Lamotte, D., Zizi, M., Missenard, Y., Hafid, M., El Azzouzi, M., Maury, R.C., Charrière, A., Taki, Z., Benammi, M., Michard, A., 2008. The Atlas system. In: Michard, A., Saddiqi, O., Chalouan, A., Frizon de Lamotte, D. (Eds.), Continental Evolution: The Geology of Morocco, Lecture Notes in Earth Sciences. Springer-Verlag, Berlin, pp. 133–202.
Gidon, M., 1997. Les chaînons subalpins au Nord-Est de Sisteron et l'histoire tectonique de la nappe de Digne. Géol. Alpine 73, 23–57.
Gidon, M., Pairis, J.-L., 1992. Relations entre le charriage de la Nappe de Digne et la structure de son autochtone dans la vallée du Bès (Alpes de Haute-Provence, France). Eclogae Geol. Helv. 85 (2), 327–359.
Godet, A., Bodin, S., Föllmi, K.B., Vermeulen, J., Gardin, S., Fiet, N., Adatte, T., Berner, Z., Stüben, D., Van de Schootbrugge, B., 2006. Evolution of the marine stable carbon-isotope record during the early Cretaceous: a focus on the late Hauterivian and Barremian in the Tethyan realm. Earth Planet. Sci. Lett. 242, 254–271.
Grasby, S.E., Them, T.R., Chen, Z., Yin, R., Ardakani, O.H., 2019. Mercury as a proxy for volcanic emissions in the geologic record. Earth Sci. Rev. 196, 102880.
Gréselle, B., Pittet, B., 2010. Sea-level reconstruction from the Peri-Vocontian Zone (South-east France) point to Valanginian glacio-eustasy. Sedimentology 57, 1640–1684.
Gröcke, D., 2002. The carbon isotope composition of ancient CO2 based on higher-plant organic matter. Philos. Trans. R. Soc. A Math. Phys. Eng. Sci. 360, 633–658.
Haccard, D., Beaudouin, B., Gigot, P., Jorda, M., 1989. Notice Explicative, Carte géologique France (1/50000) Feuille La Javie (918). In: BRGM, Orléans, p. 152.
Hamon, Y., Merzeraud, G., 2007. C and O isotope stratigraphy in shallow-marine carbonate: a tool for sequence stratigraphy (example from the Lodève region, peritethian domain). Swiss J. Geosci. 100 (1), 71–84.
Hayes, J.M., Strauss, H., Kaufman, A.J., 1999. The abundance of 13C in marine organic matter and isotopic fractionation in the global biogeochemical cycle of carbon during the past 800 Ma. Chem. Geol. 161 (1–3), 103–125.
Hermoso, M., Le Callonnec, L., Minoletti, F., Renard, M., Hesselbo, S.P., 2009. Expression of the Early Toarcian negative carbon-isotope excursion in separated carbonate microfractions (Jurassic, Paris Basin). Earth Planet. Sci. Lett. 277, 194–203.
Hesselbo, S.P., Gröcke, D.R., Jenkyns, H.C., Bjerrun, C.J., Farrimond, P., Morgans Bell, H. S., Green, O.R., 2000. Massive dissociation of gas hydrate during a Jurassic oceanic anoxic event. Nature 406, 392–395.
Hesselbo, S.P., Jenkyns, H.C., 1995. A comparison of the Hettangian to Bajocian successions of Dorset and Yorkshire. In: Taylor, P.D. (Ed.), Field Geology of the British Jurassic. Geological Society, Bath, UK, pp. 105–150.
Hesselbo, S.P., Jenkyns, H.C., 1998. British Lower Jurassic sequence stratigraphy. In: de Graciansky, P.-C., Hardenbol, J., Jacquin, T., Vail, P.R. (Eds.), Mesozoic and Cenozoic Sequence Stratigraphy of European Basins. Special Publication Society for Sedimentary Geology, 60, pp. 561–581.
Hesselbo, S.P., Jenkyns, H.C., Duarte, L.V., Oliveira, L.C.V., 2007. Carbon-isotope record of the Early Jurassic (Toarcian) Oceanic Anoxic Event from fossil wood and marine carbonate (Lusitanian Basin, Portugal). Earth Planet. Sci. Lett. 253, 455–470.
Howard, A.S., 1985. Lithostratigraphy of the Staithes Sandstone and Cleveland Ironstone formations (Lower Jurassic) of north-East Yorkshire. Proc. Yorks. Geol. Soc. 45 (4), 261–275.
Ivimey-Cook, H.C., 1971. In: Woodland, A.W. (Ed.), The Llandbedr (Mochras Farm) Borehole. Institute of Geological Sciences, Report No. 71, pp. 87–92.
Janetschke, N., Wilmsen, M., 2014. Sequence stratigraphy of the lower Upper cretaceous Elbtal Group (Cenomanian–Turonian of Saxony, Germany). Z. Dtsch. Ges. Geowiss. 165 (2), 179–208.
Jarvis, I., Lignum, J.S., Gröcke, D.R., Jenkyns, H.C., Pearce, M.A., 2011. Black shale deposition, atmospheric CO2 drawdown, and cooling during the Cenomanian-Turonian Oceanic Anoxic Event. Paleoceanography 26, PA3201.
Jenkyns, H.C., 1988. The early Toarcian (Jurassic) Anoxic Event: stratigraphy, sedimentary, and geochemical evidence. Am. J. Sci. 288, 101–151.
Jenkyns, H.C., 2010. Geochemistry of oceanic anoxic events. Geochem. Geophys. Geosyst. 11 (Q 03004(3)), 1–30.
Jenkyns, H.C., 2018. Transient cooling episodes during cretaceous Oceanic Anoxic events with special reference to OAE 1a (Early Aptian). Philos. Trans. R. Soc. A Math. Phys. Eng. Sci. 376 (2130).
Keller, G., Berner, Z., Adatte, T., Stüben, D., 2004. Cenomanian-Turonian and δ13C, and δ18O, sea level and salinity variations at Pueblo, Colorado. Palaeogeogr. Palaeoclimatol. Palaeoecol. 211, 19–43.
Kemp, D.B., Chen, W., Cho, T., Algeo, T.J., Shen, J., Ikeda, M., 2022. Deep-ocean anoxia across the Pliensbachian-Toarcian boundary and the Toarcian Oceanic Anoxic Event in the Panthalassic Ocean. Glob. Planet. Chang. 212, 103782.
Kerckhove, C., Roux, M., 1976. Notice explicative, Carte géologique France (1/50000) feuille Castellane (971). BRGM, Orléans, 39 pp.
Korte, C., Hesselbo, S.P., 2011. Shallow marine carbon and oxygen isotope and elemental records indicate icehouse-greenhouse cycles during the Early Jurassic. Paleoceanography 26, PA4219.
Korte, C., Hesselbo, S.P., Ullmann, C.V., Dietl, G., Ruhl, M., Schweigert, G., Thibault, N., 2015. Jurassic climate mode governed by ocean gateway. Nat. Commun. 6, 10015.
Krencker, F.-N., Bodin, S., Hoffmann, R., Suan, G., Mattioli, E., Kabiri, L., Föllmi, K.B., Immenhauser, A., 2014. The middle Toarcian cold snap: trigger of mass extinction and carbonate factory demise. Glob. Planet. Chang. 117, 64–78.
Krencker, F.-N., Bodin, S., Suan, G., Heimhofer, U., Kabiri, L., Immenhauser, A., 2015. Toarcian extreme warmth led to tropical cyclone intensification. Earth Planet. Sci. Lett. 425, 120–130.
Krencker, F.-N., Fantasia, A., Danisch, J., Martindale, R., Kabiri, L., El Ouali, M., Bodin, S., 2020. Two-phased collapse of the shallow-water carbonate factory during the late Pliensbachian-Toarcian driven by changing climate and enhanced continental weathering in the Northwestern Gondwana margin. Earth Sci. Rev. 208, 103254.
Krencker, F.N., Fantasia, A., El Ouali, M., Kabiri, L., Bodin, S., 2022. The effects of strong sediment-supply variability on the sequence stratigraphic architecture: insights from early Toarcian carbonate factory collapses. Mar. Pet. Geol. 136, 105469.
Krencker, F.-N., Lindström, S., Bodin, S., 2019. A major sea-level drop briefly precedes the Toarcian oceanic anoxic event: implication for Early Jurassic climate and carbon cycle. Sci. Rep. 9, 12518.
Legarreta, L., Uliana, M.A., 1996. The Jurassic succession in west-Central Argentina: stratal patterns, sequences and paleogeographic evolution. Palaeogeogr. Palaeoclimatol. Palaeoecol. 120 (3–4), 303–330.
Léonide, P., Floquet, M., Durlet, C., Baudin, F., Pittet, B., Lécuyer, C., 2012. Drowning of a carbonate platform as a precursor stage of the early Toarcian global anoxic event (Southern Provence sub-Basin, South-east France). Sedimentology 59, 156–184.
Léonide, P., Floquet, M., Villier, L., 2007. Interaction of tectonics, eustasy, climate and carbonate production on the sedimentary evolution of an early/middle Jurassic

extensional basin (Southern Provence Sub-basin, SE France). Basin Res. 19 (1), 125–152.
Lickorish, W.H., Ford, M., 1998. Sequential restoration of the external Alpine Digne thrust system, SE France, constrained by kinematic data and synorogenic sediments. Geol. Soc. Lond., Spec. Publ. 134 (1), 189–211.
Little, C.T.S., Benton, M.J., 1995. Early Jurassic mass extinction: a global long-term event. Geology 23 (6), 495–498.
Littler, K., Hesselbo, S.P., Jenkyns, H.C., 2010. A carbon-isotope perturbation at the Pliensbachian-Toarcian boundary: evidence from the Lias Group,NE England. Geol. Mag. 147 (2), 181–192.
Mattioli, E., Pittet, B., 2004. Spatial and temporal distribution of calcareous nannofossils along a proximal–distal transect in the lower Jurassic of the Umbria–Marche Basin (central Italy). Palaeogeogr. Palaeoclimatol. Palaeoecol. 205, 295–316.
McArthur, J.M., Donovan, D.T., Thirlwall, M.F., Fouke, B.W., Mattey, D., 2000. Strontium isotope profile of the early Toarcian (Jurassic) oceanic anoxic event, the duration of ammonite biozones, and belemnite palaeotemperatures. Earth Planet. Sci. Lett. 179, 269–285.
Menini, A., Mattioli, E., Hesselbo, S.P., Ruhl, M., Suan, G., 2021. Primary v. carbonate production in the Toarcian, a case study from the Llanbedr (Mochras Farm) borehole, Wales. Geological Society, London, Special Publications 514 (1), 59–81.
Menini, A., Mattioli, E., Spangenberg, J.E., Pittet, B., Suan, G., 2019. New calcareous nannofossil and carbon isotope data for the Pliensbachian/Toarcian boundary (Early Jurassic) in the western Tethys and their paleoenvironmental implications. Newsl. Stratigr. 52 (2), 173–196.
Merino-Tomé, Ó., Della Porta, G., Kenter, J.A.M., Verwer, K., Harris, P.M., Adams, E.W., Playton, T.E.D., Corrochano, D., 2012. Sequence development in an isolated carbonate platform (Lower Jurassic, Djebel Bou Dahar, High Atlas, Morocco): influence of tectonics, eustacy and carbonate production. Sedimentology 59 (1), 118–155.
Monaco, P., 1992. Hummocky cross-stratified deposits and turbidites in some sequences of the Umbria-Marche area (central Italy) during the Toarcian. Sediment. Geol. 77, 123–142.
Morard, A., Guex, J., Bartolini, A., Morettini, E., De Wever, P., 2003. A new scenario for the Domerian-Toarcian transition. Bull. Soc. Géol. France 174, 351–356.
Mouterde, R., 1955. Le Lias de Peniche. Comunicações dos Serviços Geológicos de Portugal 36, 87–115.
Oliveira, L.C.V., Rodrigues, R., Duarte, L.V., Brasil Lemos, V., 2006. Avaliação do potencial gerador de petroleo e interpretação paleoambiental com base em biomarcadores e isotopos estaveis de carbono da seção Pliensbaquiano-Toarciano inferior (Jurassico Inferior) da região de Peniche (Bacia Lusitânica, Portugal). Bol. Geociências Petrobras 14, 207–234.
Percival, L.M.E., Cohen, A.S., Davies, M.K., Dickson, A.J., Hesselbo, S.P., Jenkyns, H.C., Leng, M.J., Mather, T.A., Storm, M.S., Xu, W., 2016. Osmium isotope evidence for two pulses of increased continental weathering linked to early Jurassic volcanism and climate change. Geology 44 (9), 759–762.
Percival, L.M.E., Tedeschi, L.R., Creaser, R.A., Bottini, C., Erba, E., Giraud, F., Svensen, H., Savian, J., Trindade, R., Coccioni, R., Frontalini, F., Jovane, L., Mather, T.A., Jenkyns, H.C., 2021. Determining the style and provenance of magmatic activity during the early Aptian Oceanic Anoxic Event (OAE 1a). Glob. Planet. Chang. 200, 103461.
Percival, L.M.E., Witt, M.L.I., Mather, T.A., Hermoso, M., Jenkyns, H.C., Hesselbo, S.P., Al-Suwaidi, A.H., Storm, M.S., Xu, W., Ruhl, M., 2015. Globally enhanced mercury deposition during the end-Pliensbachian extinction and Toarcian OAE: a link to the Karoo-Ferrar large Igneous Province. Earth Planet. Sci. Lett. 428, 267–280.
Peti, L., Thibault, N., Clémence, M.-E., Korte, C., Dommergues, J.-L., Bougeault, C., Pellenard, P., Jelby, M.E., Ullmann, C.V., 2017. Sinemurian-Pliensbachian calcareous nannofossil biostratigraphy and organic carbon isotope stratigraphy in the Paris Basin: calibration to the ammonite biozonation of NW Europe. Palaeogeogr. Palaeoclimatol. Palaeoecol. 468, 142–161.
Peti, L., Thibault, N., Korte, C., Ullmann, C.V., Cachão, M., Fibæk, M., 2021. Environmental drivers of size changes in lower Jurassic Schizosphaerella spp. Mar. Micropaleontol. 168, 102053.
Pienkowski, G., 2004. The epicontinental lower Jurassic of Poland. Polish Geological Institute Special Papers 12, 1–154.
Pieńkowski, G., Hesselbo, S.P., Barbacka, M., Leng, M.J., 2020. Non-marine carbon-isotope stratigraphy of the Triassic-Jurassic transition in the Polish Basin and its relationships to organic carbon preservation, pCO2 and palaeotemperature. Earth Sci. Rev. 210, 103383.
Pieńkowski, G., Schudack, M.E., Bosák, P., Enay, R., Feldman-Olszewska, A., Golonka, J., Gutowski, J., Herngreen, G.F.W., Jordan, P., Krobicki, M., Lathuilière, B., Leinfelder, R.R., Michalík, J., Mönnig, E., Noe-Nygaard, N., Pálfy, J., Pint, A., Rasser, M.W., Reisdorf, A.G., Schmid, D.U., Schweigert, G., Surlyk, F., Wetzel, A., Wong, T.E., 2008. Jurassic. In: McCann, T. (Ed.), The Geology of Central Europe (Volume 2): Mesozoic and Cenozoic. Geological Society Publishing House, pp. 823–922.
Pittet, B., Suan, G., Lenoir, F., Duarte, L.V., Mattioli, E., 2014. Carbon isotope evidence for sedimentary discontinuities in the lower Toarcian of the Lusitanian Basin (Portugal): sea level change at the onset of the Oceanic Anoxic Event. Sediment. Geol. 303, 1–14.
Quesada, S., Robles, S., Rosales, I., 2005. Depositional architecture and transgressive–regressive cycles within Liassic backstepping carbonate ramps in the Basque-Cantabrian basin, northern Spain. J. Geol. Soc. 162 (3), 531–548.
Rita, P., Nätscher, P., Duarte, L.V., Weis, R., De Baets, K., 2019. Mechanisms and drivers of belemnite body-size dynamics across the Pliensbachian-Toarcian crisis. R. Soc. Open Sci. 6 (12), 190494.
Röhl, H.-J., Schmid-Röhl, A., 2005. Lower Toarcian (Upper Liassic) black shales of the central european epicontinental basin: a sequence stratigraphic case study from the SW German Posidonia Shale, the deposition of organic-carbon-rich sediments: Models, mechanisms, and consequences. SEPM Special Publication No. 82, 165–189.
Rosales, I., Quesada, S., Robles, S., 2004. Paleotemperature variations of Early Jurassic seawater recorded in geochemical trends of belemnites from the Basque-Cantabrian Basin, northern Spain. Palaeogeogr. Palaeoclimatol. Palaeoecol. 203, 253–275.
Rosales, I., Quesada, S., Robles, S., 2006. Geochemical arguments for identifying second-order sea-level changes in hemipelagic carbonate ramp deposits. Terra Nova 18 (4), 233–240.
Ruebsam, W., Al-Husseini, M., 2020. Calibrating the early Toarcian (Early Jurassic) with stratigraphic black holes (SBH). Gondwana Res. 82, 317–336.
Ruebsam, W., Mayer, B., Schwark, L., 2019. Cryosphere carbon dynamics control early Toarcian global warming and sea level evolution. Glob. Planet. Chang. 172, 440–453.
Ruebsam, W., Reolid, M., Sabatino, N., Masetti, D., Schwark, L., 2020. Molecular paleothermometry of the early Toarcian climate perturbation. Glob. Planet. Chang. 195, 103351.
Ruhl, M., Hesselbo, S.P., Hinnov, L., Jenkyns, H.C., Xu, W., Riding, J.B., Storm, M.S., Minisini, D., Ullmann, C.V., Leng, M.J., 2016. Astronomical constraints on the duration of the early Jurassic Pliensbachian Stage and global climatic fluctuations. Earth Planet. Sci. Lett. 455, 149–165.
Ruhl, M., Hesselbo, S.P., Jenkyns, H.C., Xu, W., Silva, R.L., Matthews, K.J., Mather, T.A., Mac Niocaill, C., Riding, J.B., 2022. Reduced plate motion controlled timing of early Jurassic Karoo-Ferrar large igneous province volcanism. Science. Advances 8, eabo0866.
Sanei, H., Grasby, S.E., Beauchamp, B., 2012. Latest Permian mercury anomalies. Geology 40 (1), 63–66.
Scholle, P.A., Arthur, M.A., 1980. Carbon isotope fluctuations in cretaceous. Am. Assoc. Petrol. Geol. Bull. 64 (1), 67–87.
Schöllhorn, I., Adatte, T., Van de Schootbrugge, B., Houben, A.J.P., Charbonnier, G., Janssen, N.M.M., Föllmi, K.B., 2020. Climate and environmental response to the break-up of Pangea during the early Jurassic (Hettangian-Pliensbachian); the Dorset coast (UK) revisited. Glob. Planet. Chang. 185, 103096.
Silva, R.L., Duarte, L.V., 2015. Organic matter production and preservation in the Lusitanian Basin (Portugal) and Pliensbachian climatic hot snaps. Glob. Planet. Chang. 131, 24–34.
Silva, R.L., Duarte, L.V., Comas-Rengifo, M.J., 2015. Chapter 13 - Facies and carbon isotope chemostratigraphy of Lower Jurassic carbonate deposits, Lusitanian Basin (Portugal): implications and. In: Ramkumar, M. (Ed.), Chemostratigraphy. Elsevier, Oxford, pp. 341–371.
Storm, M.S., Hesselbo, S.P., Jenkyns, H.C., Ruhl, M., Ullmann, C.V., Xu, W., Leng, M.J., Riding, J.B., Gorbanenko, O., 2020. Orbital pacing and secular evolution of the early Jurassic carbon cycle. Proc. Natl. Acad. Sci. 117 (8), 3974–3982.
Suan, G., Mattioli, E., Pittet, B., Lécuyer, C., Suchéras-Marx, B., Duarte, L.V., Philippe, M., Reggiani, L., Martineau, F., 2010. Secular environmental precursors to early Toarcian (Jurassic) extreme climate changes. Earth Planet. Sci. Lett. 290 (3–4), 448–458.
Suan, G., Mattioli, E., Pittet, B., Mailliot, S., Lécuyer, C., 2008. Evidence for major environmental perturbation prior to and during the Toarcian (Early Jurassic) oceanic anoxic event from the Lusitanian Basin,Portugal. Paleoceanography 23, PA1202.
Suan, G., van de Schootbrugge, B., Adatte, T., Fiebig, J., Oschmann, W., 2015. Calibrating the magnitude of the Toarcian carbon cycle perturbation. Paleoceanography 30, PA002758.
Swart, P.K., Eberli, G.P., 2005. The nature of the δ13C of periplatform sediments: implications for stratigraphy and the global carbon cycle. Sediment. Geol. 175, 115–129.
Them, T.R., Gill, B.C., Caruthers, A.H., Gröcke, D.R., Tulsky, E.T., Martindale, R.C., Poulton, T.P., Smith, P.L., 2017. High-resolution carbon isotope records of the Toarcian Oceanic Anoxic Event (Early Jurassic) from North America and implications for the global drivers of the Toarcian carbon cycle. Earth Planet. Sci. Lett. 459, 118–126.
Them, T.R., Gill, B.C., Selby, D., Gröcke, D.R., Friedman, R.M., Owens, J.D., 2017. Evidence for rapid weathering response to climatic warming during the Toarcian Oceanic Anoxic Event. Sci. Rep. 7, 5003.
Them, T.R., Jagoe, C.H., Caruthers, A.H., Gill, B.C., Grasby, S.E., Gröcke, D.R., Yin, R., Owens, J.D., 2019. Terrestrial sources as the primary delivery mechanism of mercury to the oceans across the Toarcian Oceanic Anoxic Event (Early Jurassic). Earth Planet. Sci. Lett. 507, 62–72.
Thiry-Bastien, P., 2002. In: Stratigraphie séquentielle Des Calcaires Bajociens de l'Est de la France, 1. Université Claude Bernard –, Lyon, p. 411 pp.. PhD Thesis.
Ullmann, C.V., Boyle, R., Duarte, L.V., Hesselbo, S.P., Kasemann, S.A., Klein, T., Lenton, T.M., Piazza, V., Aberhan, M., 2020. Warm afterglow from the Toarcian Oceanic Anoxic Event drives the success of deep-adapted brachiopods. Sci. Rep. 10, 6549.
Ullmann, C.V., Szücs, D., Jiang, M., Hudson, A.J.L., Hesselbo, S.P., 2022. Geochemistry of macrofossil, bulk rock and secondary calcite in the Early Jurassic strata of the Llanbedr (Mochras Farm) drill core, Cardigan Bay Basin, Wales, UK. J. Geol. Soc. 179 (1) jgs2021-018.
Valencio, S.A., Cagnoni, M.C., Ramos, A.M., Riccardi, A.C., Panarello, H.O., 2005. Chemostratigraphy of the Pliensbachian, Puesto Araya Formation (Neuquén Basin, Argentina). Geol. Acta 3, 147–154.
van de Schootbrugge, B., McArthur, J.M., Bailey, T.R., Rosenthal, Y., Wright, J.D., Miller, K.G., 2005. Toarcian oceanic anoxic event: an assessment of global causes using belemnite C isotope records. Paleoceanography 20 (PA3008), 1–10.

Vasseur, R., Lathuilière, B., Lazăr, I., Martindale, R.C., Bodin, S., Durlet, C., 2021. Major coral extinctions during the early Toarcian global warming event. Glob. Planet. Chang. 207, 103647.
Wilmsen, M., Neuweiler, F., 2008. Biosedimentology of the early Jurassic post-extinction carbonate depositional system, central High Atlas rift basin, Morocco. Sedimentol. 55, 773–807.
Wohlwend, S., Hart, M.B., Weissert, H., 2016. Chemostratigraphy of the Upper Albian to mid-Turonian Natih Formation (Oman) – how authigenic carbonate changes a global pattern. Depositional Record 2 (1), 97–117.
Xu, W., Ruhl, M., Jenkyns, H.C., Leng, M.J., Huggett, J.M., Minisini, D., Ullmann, C.V., Riding, J.B., Weijers, J.W.H., Storm, M.S., Percival, L.M.E., Tosca, N.J., Idiz, E.F., Tegelaar, E.W., Hesselbo, S.P., 2018. Evolution of the Toarcian (Early Jurassic) carbon-cycle and global climatic controls on local sedimentary processes (Cardigan Bay Basin, UK). Earth Planet. Sci. Lett. 484, 396–411.